ROLE OF OXYGEN FREE RADICALS IN RETINAL DAMAGE ASSOCIATED WITH EXPERIMENTAL UVEITIS*

BY *Narsing Adupa Rao,* MD

INTRODUCTION

UVEITIS IS ONE OF THE MAJOR CAUSES OF LEGAL BLINDNESS IN THE United States. In over 70% of the cases, the pathogenesis remains obscure, even after extensive clinical and laboratory investigations.[1,2] Visual prognosis is worst in cases that present with severe intraocular inflammation, due primarily to retinal and uveal tissue damage in the form of vascular leakage, cystoid macular edema, and other alterations.[3,4] In such inflammations, even though T- and B-lymphocytes initiate the process, polymorphonuclear leukocytes (PMNs) and macrophages mediate amplification and perpetuation of the inflammatory process.[1]

In uveitis, tissue damage is caused by various chemical mediators derived from either plasma proteins or inflammatory phagocytic cells, PMNs, and macrophages. These mediators include arachidonic acid metabolites, proteolytic enzymes, and possibly oxygen metabolites.[1,5-9] Arachidonic acid metabolites are involved primarily in vascular permeability, chemotaxis, and amplification of inflammation. Proteolytic enzymes appear to be only a minor contributing factor in uveitis-induced retinal and uveal damage, as well as in inflammatory damage in other organs.[10,11] Attention has recently been directed to reactive oxygen metabolites (oxygen free radicals) released by PMNs and macrophages during the initial phase of inflammation.[7,8,12-17] These molecules have been implicated in amplification of inflammation and in tissue necrosis.[18-23]

In experimental animal models of uveitis, systemic treatment in the form of repeated intraperitoneal injections of antioxidant enzymes or hydroxyl radical scavengers has resulted in marked reduction in the

*From the Doheny Eye Institute, Los Angeles, California. Supported in part by Research to Prevent Blindness, Inc, New York, NY, and by grants EY0-3040, EY06953, and EY05662 from the National Eye Institute, Bethesda, Maryland.

intraocular inflammation.[18,20,24-27] The beneficial effects of such treatment are thought to be from elimination of phagocyte generated oxygen metabolites. But the antioxidants and the scavengers of oxygen metabolites can also alter other functions of phagocytes and immune cells, such as chemotaxis, antibody formation and T-cell proliferation.[28] These treatment experiments thus provide only limited evidence of in vivo generation of oxygen metabolites and of free radical mediated tissue damage in uveitis.

It has been shown in vitro that, upon phagocytosis or exposure to certain membrane-active agents, PMNs and macrophages undergo a "respiratory burst" characterized by increased consumption of oxygen, increased utilization of glucose via the hexose monophosphate shunt, and release of reactive oxygen metabolites, the principal product being superoxide anion, an inorganic free radical.[17,29-32] It has been proposed that the superoxide radical itself is poorly reactive in aqueous solution, and that the tissue damaging effects are from more reactive secondary products, including hydrogen peroxide, hypochlorous acid (HOCl) and hydroxyl radicals (Fig 1). These oxygen metabolites and free radicals have been

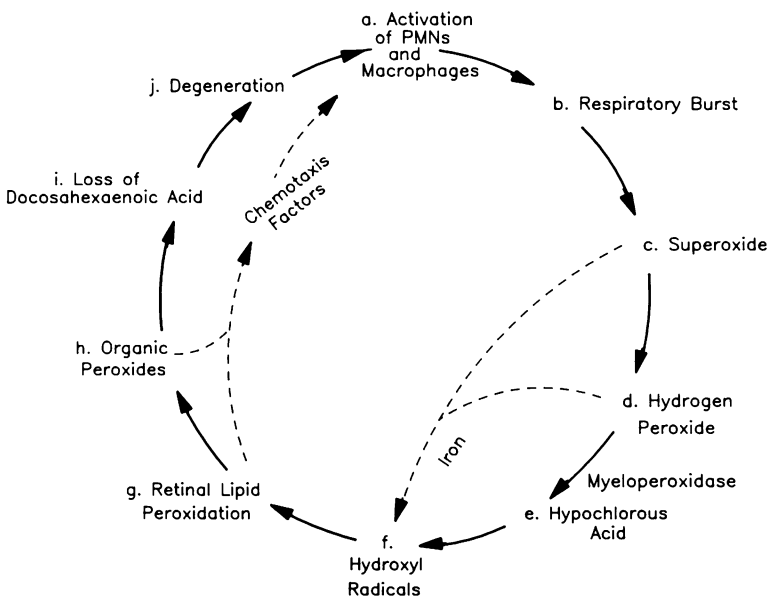

FIGURE 1

Schematic representation of oxygen metabolite generation and its effect on the retina. Once the phagocytic cells are activated, superoxide is generated along with hydrogen peroxide. These, in turn, form other reactive products resulting in retinal lipid peroxidation. Chain reaction of this peroxidation leads to formation of organic peroxides, and loss of 22:6, and eventually results in retinal degeneration. Lipid peroxidation products form chemotactic factors and thus amplify inflammation by recruiting inflammatory cells.

observed in vitro to exert direct cytotoxic effects, including lipid peroxidation of cell membranes.[7-9,14,17,33-44] But in uveitis there is no report documenting release of oxygen metabolites by the phagocytic cells and, furthermore, there is no study to show significance of these metabolites in initiating retinal or other ocular tissue damage.

The eye is unique in possessing abundant quantities of antioxidant enzymes and other antioxidant agents. The antioxidant enzymes include superoxide dismutase, catalase, glutathione peroxidase, glutathione transferase and others.[45-48] Several of these enzymes are distributed in the corneal epithelium and endothelium, lens epithelium, retina and retinal pigment epithelium. The eye also contains other antioxidants, such as ascorbate, vitamin E, ceruloplasmin, and transferrin. These agents and the enzymes are presumed to prevent the damaging effects of oxygen and its metabolites.[46-48] However, it is not known whether these agents can modify or suppress the damaging effects of oxygen metabolites if these are generated in large quantities at the site of uveitiss. As the balance between the production and catabolism of oxidants by cells and tissue is critical for maintenance of the biologic and structural integrity of the tissue, the role of free radical generation in initiation of retinal or other intraocular tissue damage should be studied in clinically relevant models of uveitis in vivo.

There are several reported animal models of uveitis.[49-55] These include the uveitis induced by organ specific ocular antigens like retinal S-antigen, rhodopsin, interphotoreceptor retinoid-binding protein (IRBP), lens protein, and others.[56-59] A second group of models consists of those induced by proteins foreign to the host, such as intravitreal injections of heterologous albumin or gamma globulins.[70-72] There is a third group of experimental models produced by intravitreal injection of cytokines, such as interleukins 1 and 2, tumor necrosis factor or complement products[73-78]; a fourth group includes intravitreal injection of bacterial products such as endotoxin,[79] and a fifth group consists of injection of xanthine and xanthine oxidase to generate oxygen radicals.[80,81] However, in the latter model, traces of endotoxin may play a role in induction of vitritis, as xanthine and xanthine oxidase are known to be contaminated by endotoxin. One major disadvantage of all the above intravitreal injection models is that the primary inflammatory response consists of an acute vitritis rather than uveitis. Thus they do not provide a clinically relevant model for uveitis studies. Of all these experimental models, uveitis induced by retinal S-antigen (EAU), rhodopsin, IRBP, and lens protein have been studied most extensively and are well characterized morphologically, clinically, and immunologically. These models offer several similarities in

clinical and pathologic features to those observed in various uveitis entities noted in humans.[57,60,82-87]

Lipid peroxidation represents one form of tissue damage. It can be initiated by oxygen or its metabolic products. In vivo, it provides a steady supply of free radicals since it is a chain reaction leading to the formation of organic peroxides. The accumulation of such peroxides can have a devastating effect on cellular vitality, leading eventually to degeneration and necrosis.[7,8,17,35-41] Docosahexaenoic acid (22:6), a major polyunsaturated fatty acid (PUFA) in photoreceptor membranes, is extremely susceptible to in vivo peroxidation. Since in biosynthetic pathways 22:6 has been established to be the end product of chain elongation and desaturation processes,[43] the disappearance of 22:6 from the retina has been considered to be due to the loss from peroxidation.[39] Depletion of this fatty acid has been demonstrated to affect visual function.[44] As the visual loss in humans with uveitis occurs mainly from retinal tissue damage, it was hypothesized that such retinal damage results from a free radical-induced peroxidation of retinal cell membranes.

In order to test the above hypothesis, generation of oxygen metabolites at the site of intraocular inflammation (retina and choroid) was investigated for the first time using chemiluminescence assay, and by a novel histochemical light and electron microscopic technique in a well-defined and highly reproducible animal model of S-antigen induced uveitis. The effect of these oxygen metabolites on the initiation of retinal damage was determined by detection of lipid peroxidation products in the retinal tissues of animals with ocular inflammation. Such retinal damage and uveal inflammation was suppressed by a free radical scavenger. Potentially, these studies could provide a basis for developing new groups of therapeutic agents with free radical scavenging properties to reduce or to eliminate retinal damage in uveitis.

MATERIALS AND METHODS

INDUCTION OF UVEITIS

Pathogen free female Lewis rats weighing 150 to 175 g (Charles River Laboratory, Inc, Wilmington, MA) were given a hind foot-pad injection of 50 μg of S-antigen in complete Freund's adjuvant containing 2 mg/ml of heat killed *Mycobacterium tuberculosis* H37 RA (DIFCO Laboratory, Detroit, MI). Several of these animals also received a tail vein injection of 1 μg of pertussis toxin (List Biological Laboratory, Campbell, CA) in 0.3 ml distilled water simultaneously on the day of S-antigen injection. Bovine retinal S-antigen was isolated according to the procedure described

by Dorey et al,[88] with minor modifications. Briefly, the antigen was precipitated from bovine retinal extract by half-saturated ammonium sulfate, then purified by gel filtration on ULTROGEL AcA 34 (IBF Biotechnics Inc, Savage, MD) followed by HA-ULTROGEL (IBF Biotechnics Inc) chromatography. The S-antigen was identified in the eluates by the Ouchterlony immunodiffusion test. The final samples of S-antigen in 0.1 M phosphate buffer were concentrated to 1 mg protein/ml by negative pressue dialysis, sterilized by filtration and lyophilized in vials containing 500 μg protein each. The S-antigen injected animals were anesthetized at various intervals, globes were enucleated and the animals were killed by intracardiac injection of pentobarbital solution. The retina and choroid were isolated from the globes for use in the following investigations. All procedures conformed to the ARVO Resolution on the Use of Animals in Research.

MORPHOMETRIC ANALYSIS

At various time periods after S-antigen injection (days 7, 9, 12, 15, 18, and 21) the globes were enucleated under anesthesia, fixed in formalin for paraffin embedding and hematoxylin and eosin (H&E) staining. The animals were killed by intracardiac injection of pentobarbital solution. All eyes were coded so that the investigator was unaware of the prior treatment until the evaluation was completed. A representative slide from each eye was selected for morphometric analysis. The slide was magnified 100× and the outline of the choroid was traced and computed for total choroidal length (perimeter) and total choroidal area using a Video Image Analysis System (Ted Pella Inc, Tustin, CA). The average choroidal thickness of each eye was obtained by dividing the total choroidal area by the total choroidal length. This value ($r = 0.9987$) correlated with 99.9% confidence limits to the mean value obtained by measuring the thickness of the choroid at 100 locations along the length of the choroid. Mean choroidal thickness values for treated and untreated animals were compared using Student's *t*-test.

ELECTRON MICROSCOPIC STUDY

Lewis rats, three in each group, sensitized with S-antigen and pertussis toxin, were anesthetized at various intervals (days 7, 9, 11, and 12) following the S-antigen injection and the globes were enucleated. The animals were then killed by intracardiac injection of pentobarbital. The globes were fixed in half-strength Karnovsky fixative. The eyes were opened and sections of the retina, with the choroid and sclera attached, were obtained from the juxtapapillary area as well as from the region

anterior to the equator. These sections were processed for ultrastructural examination. Thick sections were stained with toluidine blue. Representative ultrathin sections were prepared, stained with uranyl acetate and examined under a Zeiss 10 microscope.

DETECTION OF MYELOPEROXIDASE

Leukocytes were obtained from Lewis rats using the method described by Hirsch and Church.[89] Briefly, 0.2% glycogen was injected intraperitoneally. Four hours later, the cavity was irrigated with 20 ml of sterile Roswell Park Memorial Institute (RPMI) media containing 2 U/ml of heparin and the leukocyte-rich exudates were collected. After centrifugation, leukocytes were separated in a discontinuous gradient of Ficoll (Pharmacia, Piscataway, NJ), washed three times, and suspended in RPMI. Contaminating erythrocytes were subjected to hypotonic lysis in 3 volumes of distilled water for 30 seconds, followed by the addition of 1 volume of 3.5% NaCl solution. The leukocytes were counted using a hemacytometer.

Myeloperoxidase (MPO) was extracted from retinas and choroids homogenized in potassium phosphate buffer (50 mM, pH 6.0) containing 0.5% hexadecyltrimethylammonium bromide, similar to the procedure previously described by Williams et al.[90] The homogenates were then sonicated in an ice bath for 10 seconds, freeze-thawed three times, sonicated again and centrifuged at 40,000 × g for 15 minutes. A 0.2 ml portion of the supernatant was mixed with 2.8 ml potassium phosphate buffer containing 0.167 mg/ml of o-dianisidine dihydrochloride (Sigma Chemical Company, St. Louis, MO) and H_2O_2 (0.0005%). The increase in absorbance at 460 nm was recorded continuously for 10 minutes with a Shimadzu spectrophotometer, model UV-160 (Shimadzu Corporation, Kyoto, Japan). One unit of MPO is defined as that degrading 1 μmole of H_2O_2/minute at 25°C. A molar extinction coefficient of 1.13×10^4 for oxidized o-dianisidine was used for the calculation.

DETECTION OF SUPEROXIDE BY NITROBLUE TETRAZOLIUM TEST

Superoxide production in the uveal inflammatory infiltrate was measured by the reduction of nitroblue tetrazolium (NBT; Sigma Chemical Co). In this test, NBT is reduced to a dark blue water insoluble formazan[91] by superoxide anion. Globes obtained from animals with uveitis and from control animals without uveitis, six in each group, were dissected to obtain small fragments of choroid. The choroidal fragments were placed on glass slides and exposed to 0.1% NBT. Prior to incubation, some of the choroidal fragments were treated wtih superoxide dismutase (SOD) (1

mg/ml) or a mixture of deferoxamine mesylate and MnO_2 (0.5 mM). The slides were covered and incubated at 37°C in 5% CO_2 for 1 hour. The procedure was repeated with isolated cells from choroid to determine the location of insoluble formazan. Formazan positive cells were visualized microscopically using a blue filter.

ULTRASTRUCTURAL HISTOCHEMICAL DETECTION OF H_2O_2 PRODUCTION IN UVEITIS

The electron microscopic method of Briggs et al[92] was utilized to detect the presence of H_2O_2 in the ocular inflammation. The principle of the method includes the reaction of cerium ion with H_2O_2 in the tissue to form electron dense deposits of cerium perhydroxide, which can be detected by electron microscopic examination. Six female Lewis rats injected with S-antigen were killed on day 14; the globes were enucleated and fixed for 10 minutes in cold 2% glutaraldehyde solution buffered with 0.1 M sodium cacodylate, pH 7.3. The globes were dissected to obtain small blocks of tissue representing cornea, ciliary body and iris, retina and choroid. These tissue samples were washed and then incubated in a medium consisting of 1 mM 3-amino-1,2,4-triazole (Sigma Chemical Co) in 0.1 M tris maleate buffer, pH 7.5, for 10 minutes. Tissue blocks were then transferred to an incubating medium containing 1.0 mM cerium chloride, 0.8 mM NADH (Sigma Chemical Co) or NADPH (Sigma) and 10 mM 3-amino-1,2,4-triazole in 0.1 M tris maleate buffer for 12 minutes at 37°C. These samples were then postfixed in cold 1% osmium tetroxide in vernal buffer solution for 1 hour. The samples were dehydrated and embedded in Spurr resin.

For positive controls, the uterine endometrium from the above animals was processed as described for the ocular tissues. For negative controls, globes and uterine tissues were similarly processed without the addition of the NADPH substrate in the incubation medium.

CHEMILUMINESCENCE ASSAY FOR DETECTION OF OXYGEN METABOLITES

The luminol amplified chemiluminescence (LAC) is an assay utilized for measuring oxygen metabolites and lipid radicals generated by phagocytes. The ultraweak luminescence emitted by these radicals is chemically amplified to produce sufficient photons to be counted in a liquid scintillation analyzer. Utilizing this principle, oxgyen free radicals in the inflamed choroid and retina were measured by the method of Trush et al,[93] with slight modification. A stock solution of luminol (5-amino 2,3-dihydro-1,4-phthalazinedione, Sigma Chemical Co) was prepared by first dissolving 1 mg of luminol in 100 μl of dimethyl sulfoxide (Sigma Chemical Co) and then diluting it to 10 ml with 0.01 M phosphate buffered saline (pH 7.4).

Exactly 400 μl of the stock solution was diluted to 200 ml with 0.01 M phosphate buffered saline to provide the working solution, the final concentration of luminol in the working solution being 0.2 μg/ml.

Six retinas plus choroids dissected from the globes of animals injected with S-antigen and pertussis toxin were placed in polypropylene counting vials and 10 ml of luminol working solution was added immediately before counting. The vials were then capped and the LAC was counted on a Packard 1500 Liquid Scintillation Analyzer with operating mode set in single photon counting. This mode sets the two photomultiplier tubes in out-of-coincidence counting, thus maximizing the counting efficiency of weak photon emission. All polypropylene vials and solutions used were dark-adapted for a period of time to reduce background in each set of experiments. Samples were counted for 1 minute, immediately after mixing with luminol, and the counting was repeated for several cycles to measure either the decay of radicals or kinetics of the suppression in the case where antioxidant enzymes or radical scavengers were added. These experiments were conducted in triplicate utilizing a total of 18 globes for each procedure. For control, retinas and choroids obtained from animals without S-antigen immunization were similarly processed.

CHARACTERIZATION OF LAC

The presence and relative contribution of superoxide anion, hydrogen peroxide, and hydroxyl radicals in LAC were examined. The suppression of LAC by the addition of 5400 U of superoxide dismutase (from bovine erythrocytes, 3150 U/mg solid; 3250 U/mg protein, Sigma Chemical Co), 11,000 U of catalase (from bovine liver, 11,000 U/mg solid; 14,000 U/mg protein, Sigma Chemical Co), 10 mM of D-mannitol (99% pure, Sigma Chemical Co), and 10 mM of deferoxamine mesylate (CIBA Pharmaceutical Company, Summit, NJ) were measured. The dosage of antioxidant enzymes, D-mannitol and deferoxamine were selected on the basis of a previous report.[94] In a typical experiment, the briefly minced retinas and choriods from a total of 12 eyes were thoroughly mixed before dividing into two vials. This manipulation assured similar magnitude of LAC counts in the two vials before adding scavenger to one vial. The extent of the additive-generated suppression was established in each case by comparing the LAC counts with and without added scavenger or antioxidant enzyme.

DETECTION OF LIPID PEROXIDATION PRODUCTS

Retinal and choroidal tissues dissected from various groups of animals that were killed at different time periods following S-antigen injection

(days 7, 9, 12, 15, and 18) were analyzed for presence of lipid peroxidation products. The biochemical indices for lipid peroxidation consisted of detection of conjugated dienes (CD), malondialdehyde (MDA), fluorochromic proteins containing lipids with the Schiff base structures, and hydroperoxides, and loss of 22:6. All parameters were also assessed quantitatively except for hydroperoxides.

1. Determination of CD: The globes from the uveitis and control animals were dissected to obtain retina and choroid. The lipids from these tissues were extracted by the method of Folch et al.[95] For each determination (done in triplicate), retinas and choroids from two eyes were combined (total of six eyes) and homogenized in 2 ml of chloroform/methanol (2:1) containing 0.5 mg of butylated hydroxytoluene (BHT) per 100 ml of solvent. After homogenization, the contents were vortexed for 1 minute to ensure complete extraction before 0.4 ml of water was added to wash the organic layer. The mixture was then centrifuged at 3000 rpm for 5 to 10 minutes to separate the layers and the chloroform-methanol layer was collected. Solvents were then evaporated under nitrogen and the residue was dissolved in 1 ml of ethanol (anhydrous "photrex" grade, J.T. Baker Chemical Co, Phillipsburg, NJ) for UV measurement. A Shimadzu spectrophotometer model UV-160 was used to record the absorption range of 200 to 400 nm. For estimating CD, absorbance at 233 nm was measured and molar extinction coefficient of 25,200 was used to calculate the quantity of CD produced.[96-100]

2. Determination of MDA: Quantitation of MDA in the tissues was carried out by the method of Uchiyama and Mihara.[101] Two retinas and choroids were homogenized in 1.15% potassium chloride (KCl) to make up to 10% w/v tissue homogenate. To this suspension, 3 ml of 1% phosphoric acid and 1 ml of 0.6% thiobarbituric acid were added and the mixture was heated in a 95°C water bath for 45 minutes. After cooling to room temperature. the reaction mixture was extracted with 4.0 ml of n-butanol ("photrex" grade, J.T. Baker Chemical Co). The butanol layer was then separated by centrifugation. The absorbance of the butanol phase was measured at 535 nm by a Shimadzu UV-160 spectrophotometer. These experiments were also conducted in triplicate. For controls, retinas and choroids from naive animals were similarly processed and analyzed in triplicate for both CD and MDA.

For verifying the molar extinction coefficient used, an MDA standard was prepared by the hydrolysis of 1,1,3,3-tetraethoxypropane (Sigma Chemical Co).[102] A standard solution of 1,1,3,3-tetraethoxypropane (1×10^{-5} M) was prepared by diluting 0.05 ml of 10 mM solution to 50 ml and the absorption spectrum was recorded. With the adjustment of purity of the standard, the molar extinction coefficient obtained (15,600) was the

same as that previously reported by other investigators.[103,104]

3. Determination of fluorescent chromolipid: Modification of a procedure described by Ward et al[37] for detection of chromolipids was used. Briefly, two retinas and choroids were homogenized for 1 minute in 2 ml of 0.05 M phosphate buffer containing 0.2 ml of 5 mM EDTA. Following homogenization, the mixture was extracted with 6 ml chloroform/methanol (2:1) by vortexing for 1 minute. About 6 ml of water was added and the mixture centrifuged to separate the layers. The fluorescence emissions on both the aqueous and chloroform/methanol layers were determined using excitation at 360 nm and emission at 430 nm.[105,106] The measurement was carried out using an Aminco-Bowman Spectrophotofluorometer. A quinine sulfate solution, 1 μg/ml in 0.1 N H_2SO_4, was used as standard. The procedure was carried out in triplicate utilizing retina and choroid obtained from S-antigen injected animals at various time intervals, including days 7, 9, 12, 15, 18, and 21. For controls, retinas and choroids from naive animals were similarly processed and measured in triplicate.

4. Detection of hydroperoxide-derived hydroxy fatty acid and determination of loss of docosahexaenoic acid: Total lipids from six retinas and choroids were obtained as described for the determination of CD. The crude lipid was then reduced by $NaBH_4$ (98% pure, Sigma Chemical Co). The reaction was carried out by adding about 50 mg of $NaBH_4$ to the lipids dissolved in 1.5 ml of methanol. The mixture was then stirred at room temperature for 15 minutes. A second portion of $NaBH_4$, about 25 mg, was added and stirring was continued for an additional 15 minutes. At the end of this period, 1.5 ml of water was added to decompose excess $NaBH_4$. The reaction mixture was extracted with 2 ml of chloroform and was centrifuged to separate the layers. The extraction was repeated once more. The pooled organic layer was freed from chloroform to leave crude reduced lipids as residue.

A transesterification to release and methylate fatty acid from the complex lipids was carried out by reacting the lipids with METH-PREP II (0.2 M m-trifluoromethylphenyl-trimethylammonium hydroxide in methanol, Alltech Associates, Inc, Deerfield, IL) using the method of van Kujik et al.[107] This procedure has been shown to give quantitative conversion of phospholipids and triglycerides to fatty acid methyl esters.[107,108] In a typical experiment, to a solution of crude lipids dissolved in 0.2 ml of methanol, 0.3 ml of METH-PREP II was added. The reaction mixture was then stirred at room temperature for 30 minutes. At the end of this period, 0.8 ml of water was added and the mixture was then extracted twice with 2 ml each of ethyl acetate. The organic layer was separated by centrifugation, pooled and evaporated under nitrogen to obtain un-

changed and hydrox esters.

To confirm the presence of hydroxy fatty acid in the tissue, both thin layer chromatography (TLC) and gas chromatography (GC) were used. TLC was carried out using precoated silica gel G plates (0.25 mm thick, Analtech, Inc, Newark, DE) and a solvent system consisting of petroleum ether/diethyl ether/acetic acid (70:30:1). The spots on the plates were visualized by dipping in a solution of 3% cupric acetate in 8.5% phosphoric acid and then charring at 140°C. A preparative scale TLC was also carried out to concentrate hydroxy fatty acids from tissues for GC/mass spectrometry (GC/MS) runs. In this preparation, a larger amount of sample was spotted continuously across the plate; after elution the positions of spots (or streaks) were located by exposing the plates to iodine vapor. The areas on the plates corresponding to hydroxy fatty acids were then scraped off and extracted with methanol to remove the desired material from the plate.

For running GC, total fatty acid methyl esters, without prior TLC separation, were used. The hydroxy fatty acid methyl esters were derivatized by adding 20 to 30 μl of N,0-bis (trimethylsilyl) trifluoroacetamide (BSTFA; Pierce Chemical Company, Rockford, IL) to convert hydroxy groups to trimethylsilyl ethers, thus facilitating the chromatography of hydroxy fatty acid methyl esters. Gas liquid chromatography of the samples was performed on a Hewlett Packard Gas Chromatograph Model 5730A equipped with a flame ionization detector. For determining the composition of the fatty acids, a fused silica megabore column, 30 m × 0.53 mm inner diameter, coated with 1 μ thickness of liquid phase DB-225 (J and W Scientific, Folsom, CA) was used. The column was run with a temperature program of 180°C to 220°C (rising rate, 2°C/minute) with both injector and detector temperature at 250°C. GC reference standards (Nu Check Prep, Inc, Elysian, MN) were used to confirm the identity of fatty acid methyl esters. For analyzing the trimethylsilyl ether of hydroxy fatty acids, a nonpolar megabore column, 30 m × 0.53 mm inner diameter coated with 1 μ thickness of phase DB-1 (J and W Scientific) was used. Column temperature was programmed from 180°C to 250°C with a rising rate of 4°C/minute, and both detector and injector were kept at 250°C. Data acquisition was performed by a Perkin Elmer 3600 series computer.

Electron impact GC/MS was carried out on a Hewlett Packard Gas Chromatograph Model 5890A coupled with a Hewlett Packard mass selective detector model 5970. The data acquisition was performed by Hewlett Packard 9000 series Model 300 computers operated through a Hewlett Packard 59970 MS Chemstation. The gas chromatograph was equipped

with a Hewlett Packard fused silica capillary column (12.5 m × 0.20 mm inner diameter) coated with cross-linked methyl silicone gum (0.33 μ thickness). The injection port temperature was 250°C, and the column temperature was programmed from 180°C to 250°C with a rising rate of 4°C/minute. The electron voltage of the detector was set at 70 eV.

TREATMENT OF EXPERIMENTAL UVEITIS BY HYDROXYL RADICAL SCAVENGER

Eighteen Lewis rats injected with 50 μg of S-antigen in complete Freund's adjuvant were divided into three groups. A group of six animals received subcutaneous implantation of an osmotic pump (Alza Corp, Palo Alto, CA) containing 2 ml of deferoxamine mesylate, 250 mg/ml, which is a well known hydroxyl radical scavenger.[28] The dosage was selected on the basis of previous reports.[24,28] A second group of six animals similarly received 2 ml of iron-saturated deferoxamine mesylate, 250 mg/ml, in an osmotic pump. The third group of animals received similar osmotic pumps containing 2 ml of normal saline solution. The above treatment procedures were carried out 1 week after S-antigen administration. All of these animals were killed on day 16, the globes were enucleated, fixed in 4% formaldehyde solution and processed for paraffin embedding. About 8-μm thick sections were cut and stained with H&E. These sections were examined for retinal damage and the thickness of the choroid was determined by morphometric analysis, as described previously.

RESULTS

In the present study, virtually all Lewis rats sensitized with S-antigen developed uveitis. The experimental disease was characterized by the appearance of conjunctival hyperemia and by cells and flare in the anterior chamber and vitreous. Several of these animals showed hypopyon and a few animals developed hyphema. These signs became apparent on day 9 or 10.

MORPHOMETRIC ANALYSIS

The choroidal thickness in naive animals was 12.37 ± 0.52 μ. Animals injected with S-antigen and sacrificed at various time periods after injection showed choroidal thickness of 11.91 ± 0.52 μ on day 7, 13.08 ± 0.47 μ on day 9, 46.55 ± 15.04 μ on day 12, 54.70 ± 6.70 μ on day 15, 32.84 ± 6.04 μ on day 18, and 23.93 ± 3.15 μ on day 21. Statistical analysis (Student's *t*-test) revealed significantly greater choroidal thickness in animals with uveitis when compared with that of controls, beginning on day 9 ($P < 0.05$) (Table I).

TABLE I: MORPHOMETRIC ANALYSIS OF UVEAL INFLAMMATION EXPRESSED AS CHOROIDAL THICKNESS IN MICRONS

GROUP OF ANIMALS (6 IN EACH)	ENUCLEATION AFTER S-ANTIGEN INJECTION (DAYS)	CHOROIDAL THICKNESS	*P* VALUE COMPARED TO CONTROLS
Controls	—	12.37 ± 0.52	
Exp 1	7	11.91 ± 0.52	> 0.05
Exp 2	9	13.08 ± 0.47	< 0.05
Exp 3	12	46.55 ± 15.04	< 0.01
Exp 4	15	54.70 ± 6.70	< 0.01
Exp 5	18	32.84 ± 6.04	< 0.01
Exp 6	21	23.93 ± 3.15	< 0.01

During the initial stages of inflammation on day 9, a mild choroidal infiltrate consisting primarily of PMNs was noted. The overlying retina was relatively well preserved but showed focal degeneration of outer segments, along with edema and necrosis of other retinal cells (Fig 2A). At the peak of the inflammation, on day 12, the infiltrate was markedly increased in the choroid as well as within the retina, which showed necrosis and loss of outer segments (Fig 2B and C). The cellular infiltrate still consisted primarily of PMNs. During the later period (day 21), the inflammatory infiltrate was reduced and the retina was atrophic and gliotic (Fig 2D). At this stage the infiltrate was made up mostly of mononuclear cells.

ELECTRON MICROSCOPIC FINDINGS

Ultrastructural examination of the retina and choroid disclosed intact photoreceptors and other retinal cells during the initial phase of inflammation, except at the site of focal inflammatory cell infiltration (Fig 3A). The inflammatory cells were mostly PMNs. The photoreceptor outer segments located adjacent to the PMNs showed disarray and disorganization of discs and of the cellular membranes (Fig 3B and C). At the peak of inflammation, on day 12, these structures were markedly swollen and disrupted (Fig 3D). During this period, the retinal damage was associated with the infiltrating PMNs or macrophages. Fibrinous material and collections of erythrocytes were also noted. The retinal pigment epithelium was necrotic in the specimens obtained on days 10 to 12.

MEASUREMENT OF PMN CONTENT USING MPO AS A MARKER

For the extraction of MPO from the retinas and choroids, the previously established method for inflamed skin was successfully adapted.[109] The o-dianisidine color reaction utilized in the present assay was also carried out with commercially available pure horseradish peroxidase to assure the

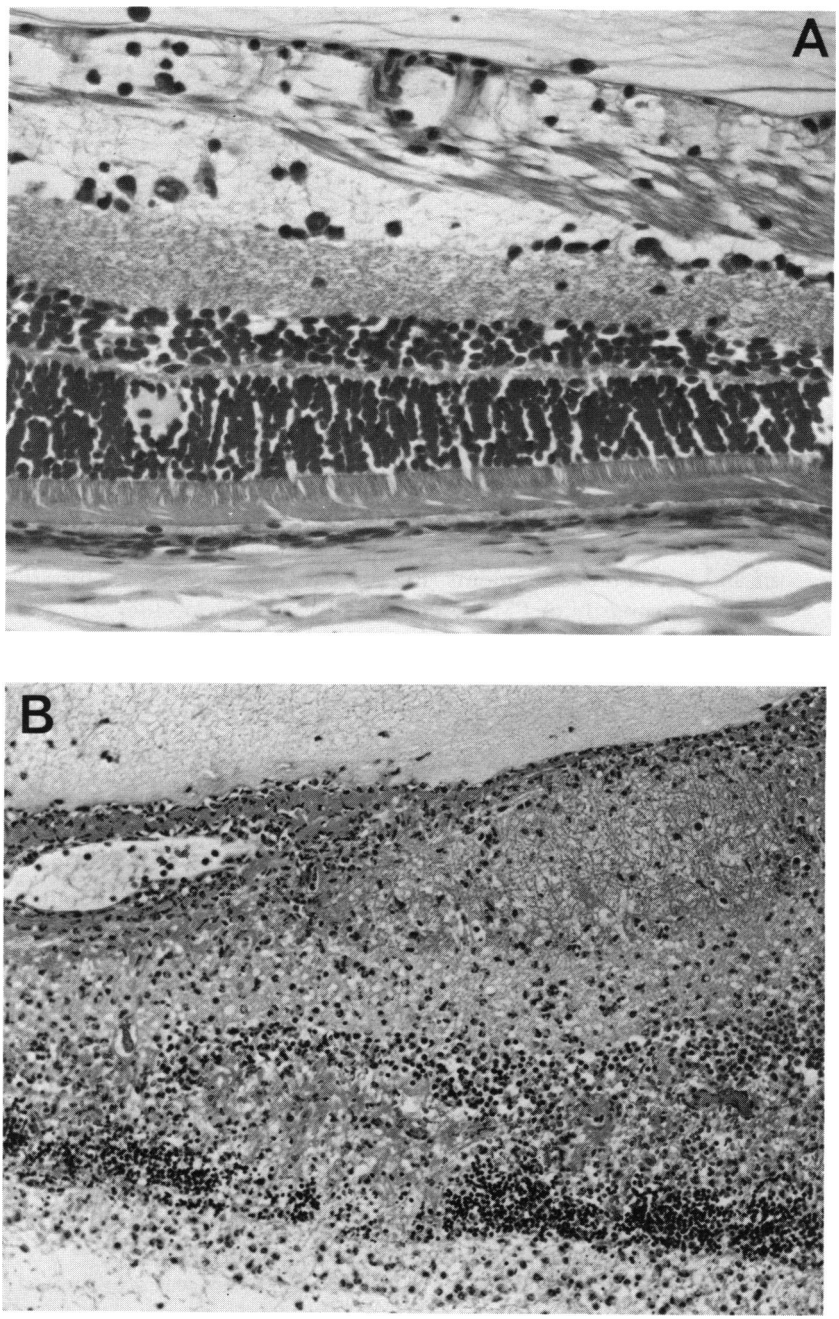
A
B

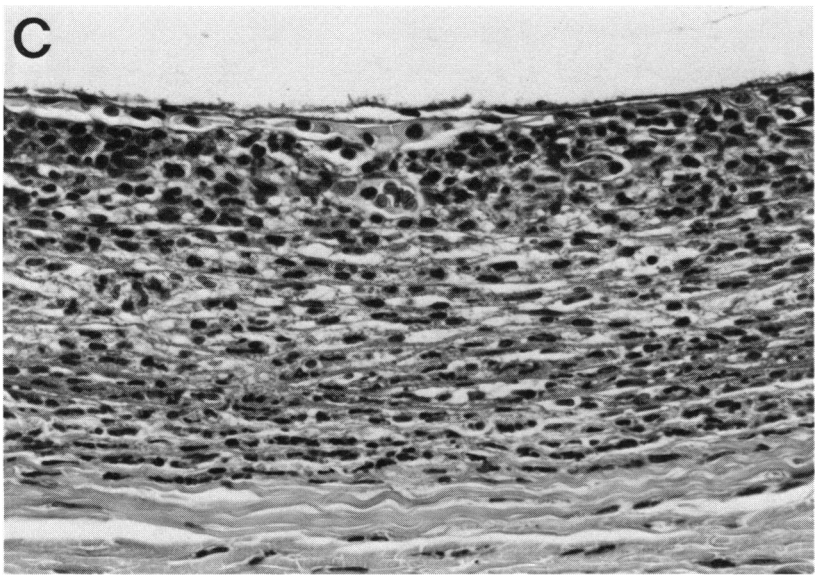

FIGURE 2

Light microscopic examination shows mild thickening of retina, occasional mononuclear inflammatory cells and eosinophilic exudate on the outer nuclear layer in the initial stages of uveitis (A, day 9, H&E, ×560), when compared with later stages of uveitis (B, day 12, H&E, ×260). Note the marked retinitis and retinal damage and choroidal inflammation (C, H&E, ×600) during this period. On day 21 (D) there is a reduction in the choroidal thickness; the outer retinal layers are absent and there is atrophy of the inner nuclear layer (H&E, ×600).

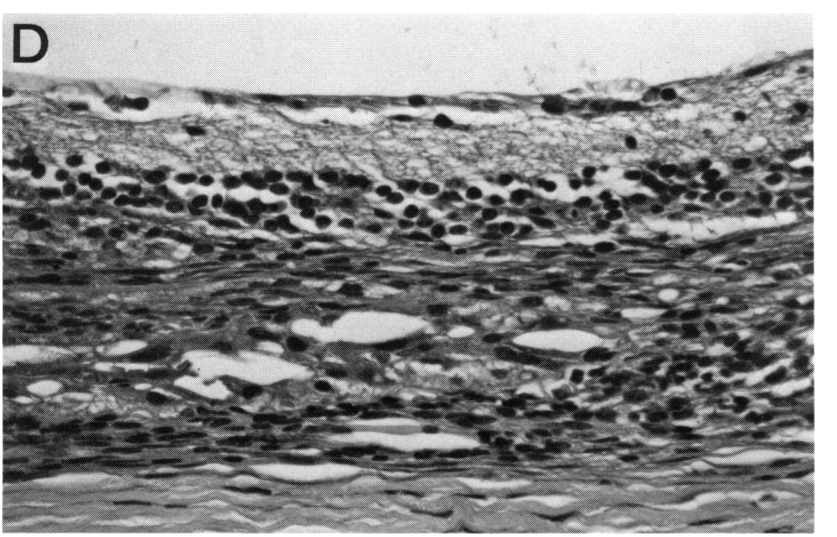

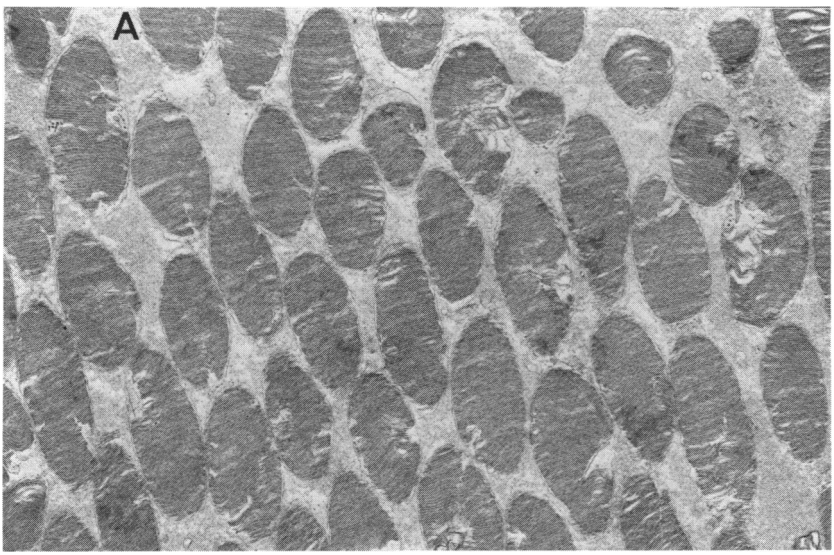

FIGURE 3

Electron microscopic changes in EAU at various time intervals. Note relatively well preserved photoreceptors on day 7 after S-antigen injection (A) (×9600). On day 9, disarray of outer segment discs is noted adjacent to the site of PMN infiltration (B) (×23,000). Disorganization and disruption of outer segments are prominent (day 11) at the site of PMN infiltration (C) (×9200). Note relatively well preserved photoreceptor outer segments located away from the PMNs. On day 12 there was marked disorganization and disruption of photoreceptor outer segments (D) (×9200).

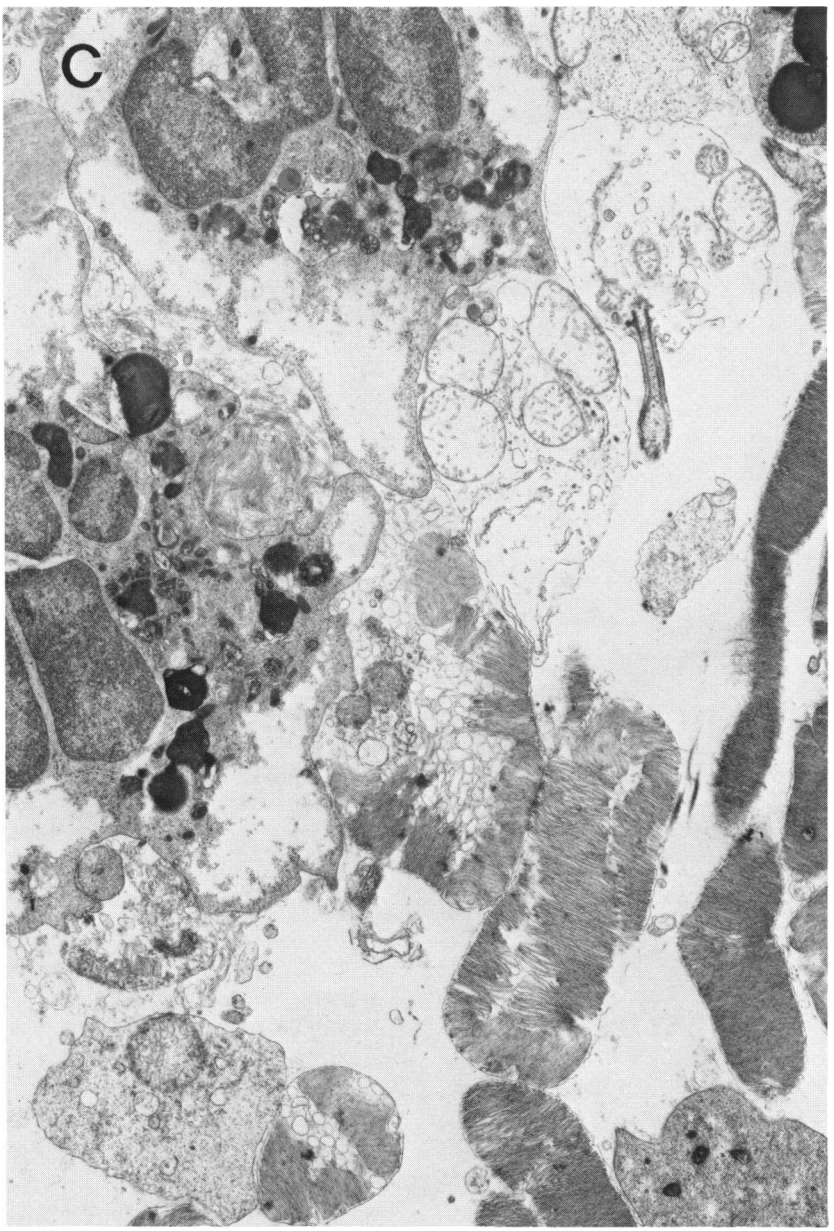
C

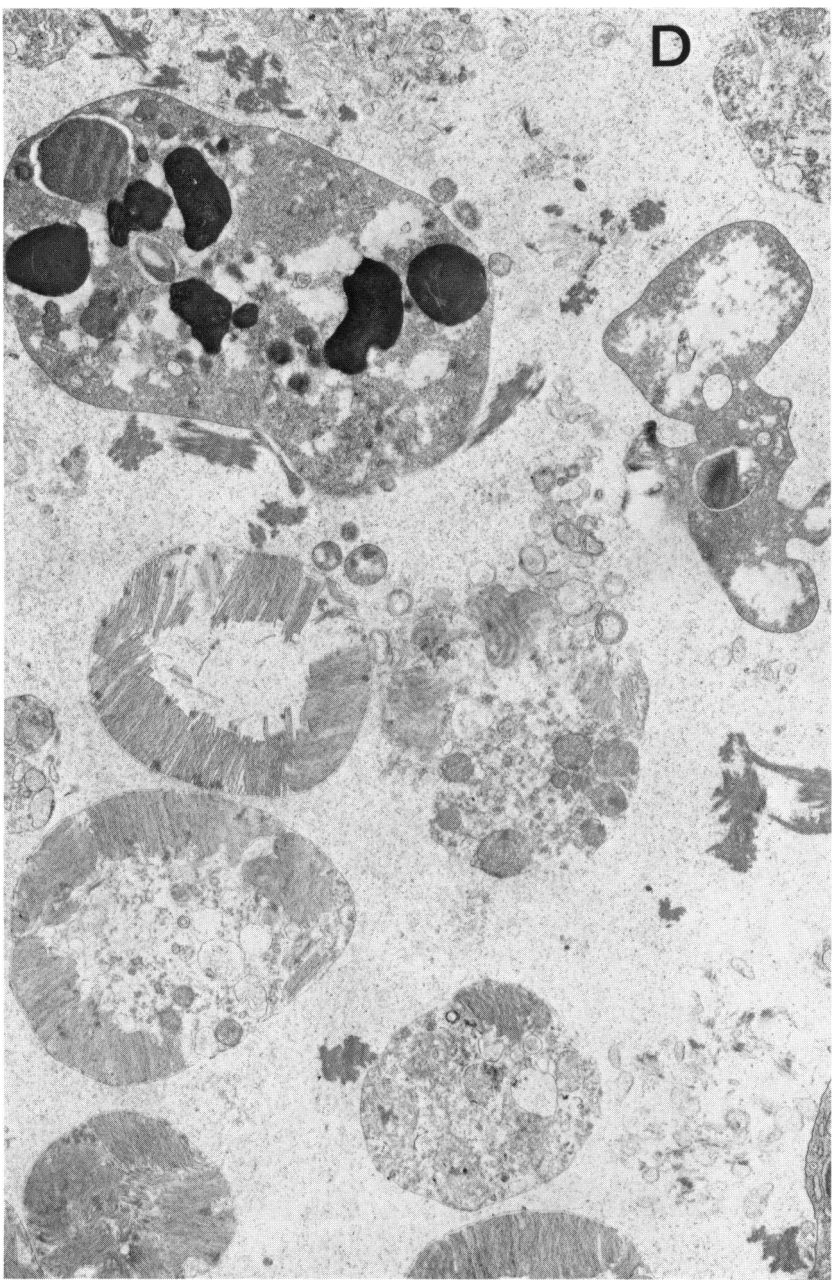
D

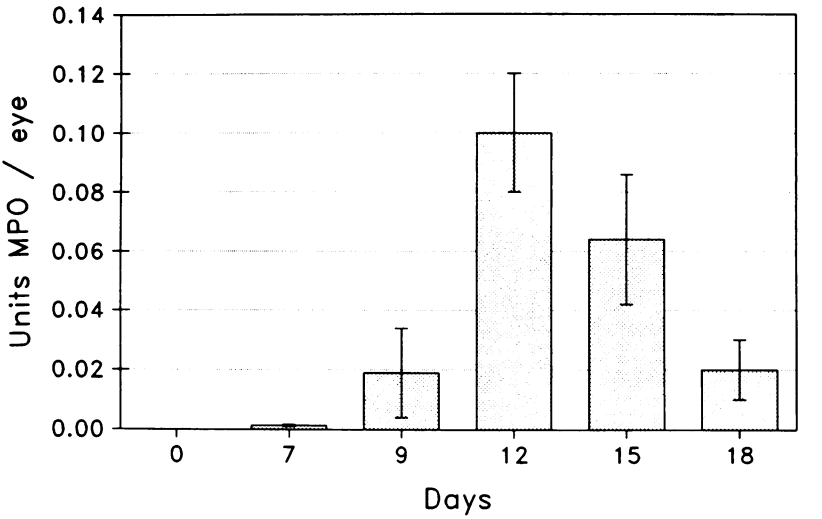

FIGURE 4
Change in the level of MPO during the development of EAU. MPO was determined at various time intervals following immunization and was expressed as MPO units/retina and choroid. Results are shown as mean ± SD (n = 3) and retina and choroid from one eye was used for one measurement. The zero time point where no MPO activity was detected was taken as the control level.

validity of the method.[110] Using isolated rat peritoneal PMNs, a linear correlation between MPO activity and number of PMNs was established. This series of experiments also gave the MPO U/10^6 PMNs to be 0.8, a value similar to that published by other investigators.[109,111,112]

The study of the time course of MPO activity, thus PMN content of tissues, during the development of the uveitis is shown in Fig 4. On day 7 there was only minimal elevation of MPO activity. Beginning with the onset of disease at day 9 postimmunization, there was a sharp increase to a maximum at day 12, and then the activity decreased relatively slowly to day 18, at which time the level of MPO activity was similar to that noted on day 9.

DETECTION OF SUPEROXIDE

The choroidal tissues obtained from experimental animals revealed positive reaction consisting of the blue staining granules that were located intracellularly (Fig 5A and B). Most of these positive cells appeared to be PMNs. Several mononuclear cells with abundant cytoplasm were also positive. Positive cells containing the blue granules were not present in

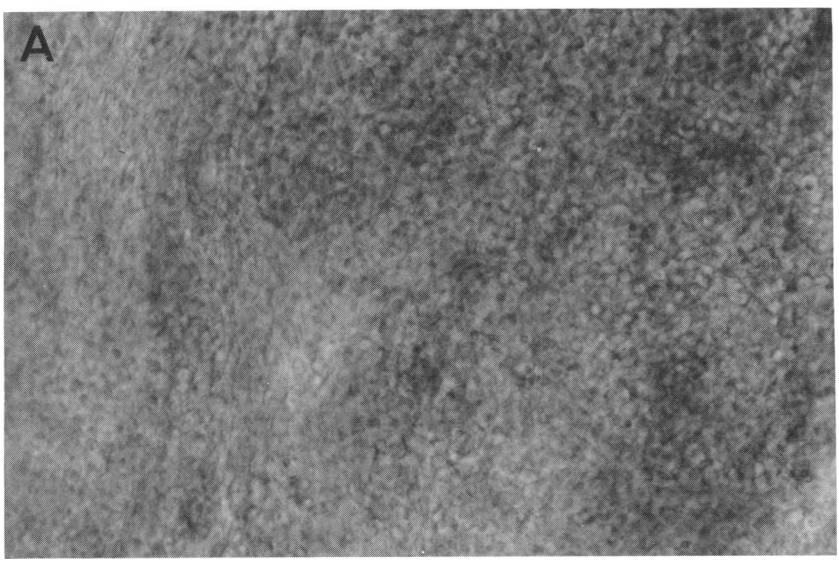

FIGURE 5

Note formazan blue positive cells in the choroidal infiltrate (A, ×40). Note presence of intracellular positive reaction products in the inflammatory cells (B, ×1000). Note absence of reaction product in the choroid treated with deferoxamine-MnO_2 (C, ×40). Absence of reaction products in the deferoxamine-MnO_2 treated uvea (D, ×1000).

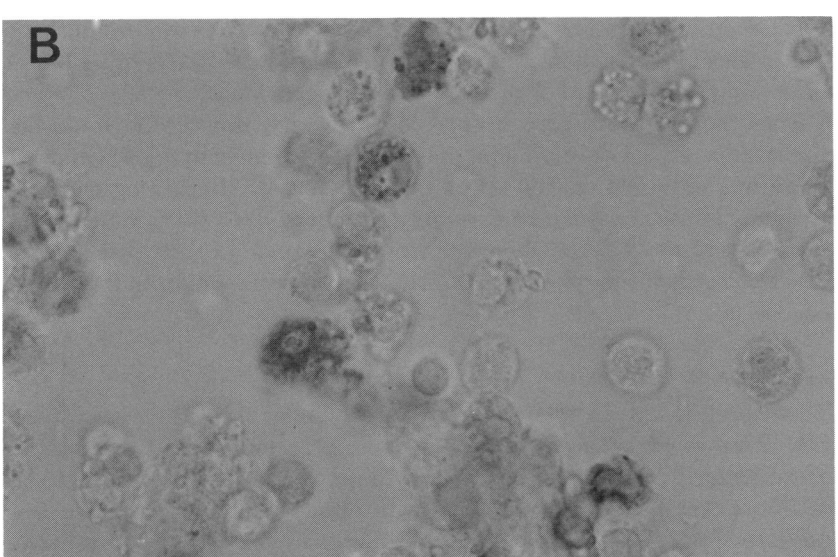

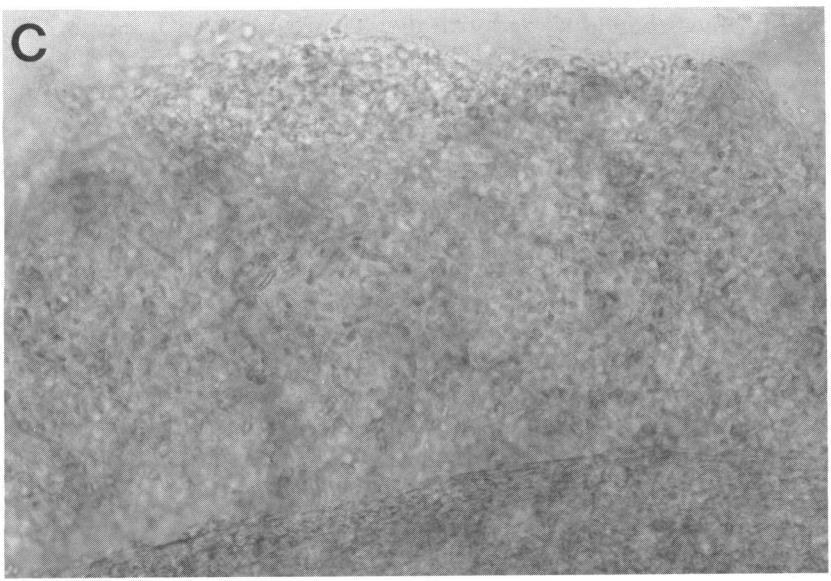
C

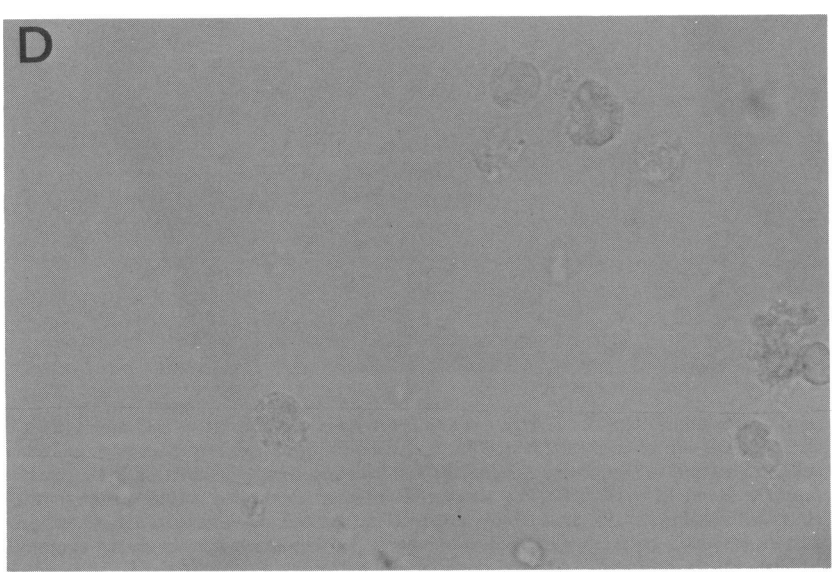
D

the inflamed choroid treated with the deferoxamine-MnO_2 mixture (Fig 5C and D). However, the inflamed choroid treated with SOD did show positive reaction products in the inflammatory infiltrate.

ULTRASTRUCTURAL HISTOCHEMICAL LOCALIZATION OF HYDROGEN PEROXIDE

In the S-antigen injected group (animals with uveoretinitis), electron dense-deposits of cerium perhydroxide were seen along the plasma membrane of the corneal epithelium. Similar deposits were seen diffusely along the basal region of the corneal endothelium. Massive electron-dense granular deposits were present along the plasma membrane of infiltrating phagocytes in the retina and uvea (Fig 6A and B). Similar deposits were also noted in the intravascular leukocytes, but there were many more such granules in the extravascular spaces (Fig 6C and D). Apical portions of the retinal pigment epithelium cells also showed these electron dense deposits.

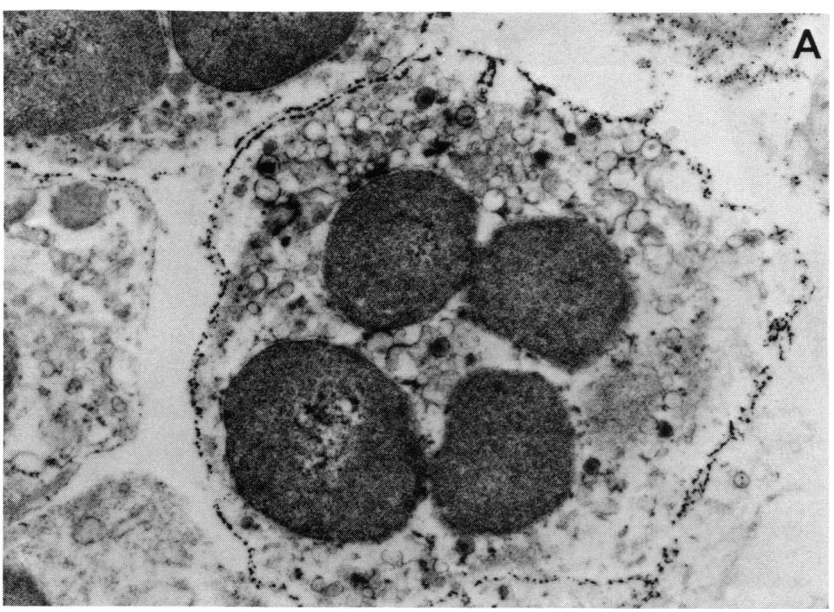

FIGURE 6

A: Electron dense deposits of H_2O_2 reaction products are present on cell membranes of PMNs at the site of retinitis (×21,000). B: Inflamed retina exhibits disruption of retinal cells, infiltrating inflammatory phagocytes and electron dense deposits of H_2O_2 reaction products (*arrow*) (×6000). C: The section of inflamed retina and retinal vessel showing abundant numbers of electron dense deposits on the cell membrane of emigrated phagocytes (×6000). D: Higher magnification shows the deposits primarily on the abluminal surface of the vessel and in the extravascular and extracellular areas of the inflamed retina (×13,000).

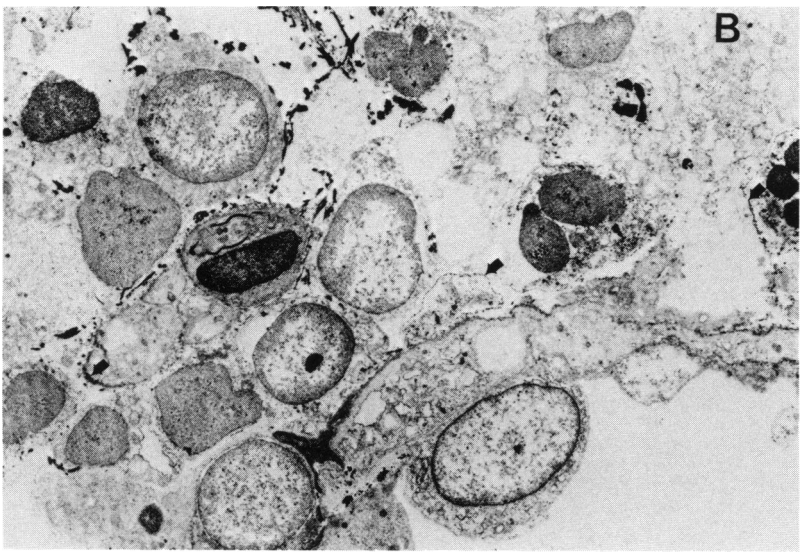
B

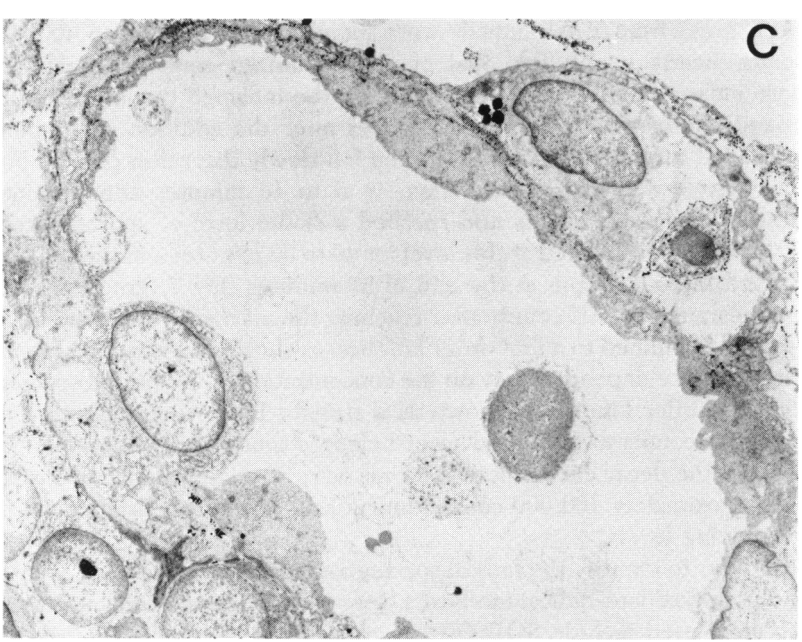
C

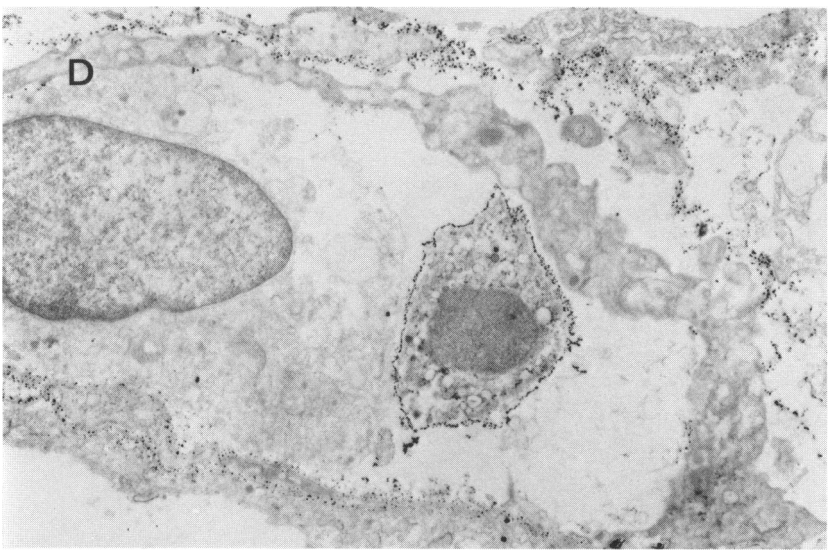

LUMINOL AMPLIFIED CHEMILUMINESCENCE

The LAC was measured on day 12 after S-antigen injection. The retina and choroid from EAU animals were found to give 300,000 to 400,000 counts, nearly twenty-fold that of nonimmunized control animals. In these measurements, the LAC counts for the inflamed tissues generally peaked approximately 12 to 19 minutes after the addition of luminol, proceeded through a plateau, and then fell slowly thereafter (Fig 7). For the controls without immunization, in 5 to 10 minutes after luminol addition, the LAC counts also reached a stable level of approximately 21,000 counts, remained at this level for 40 to 50 minutes and then slowly climbed to 25,000 cpm at the end of 50 minutes (Fig 7, group 4). The disappearance of LAC counts after reaching the maximum appeared to be linear and confined to a first order kinetics, as shown in Fig 8. The rate of disappearance depended only on the concentration of the radical species. The first order kinetics is shown as a straight line, when logarithm of remaining counts were plotted against elapsed time (Fig 8). As also shown in Fig 7, the decay curves between runs were strikingly similar, decreasing approximately 100,000 counts/hour for all of the runs, regardless of the starting levels.

In order to identify the radical species contributing to the LAC counts, various antioxidant-radical inhibitors were added. The antioxidant-radical inhibitors used include SOD (Fig 9), catalase, D-mannitol (Fig 10) and

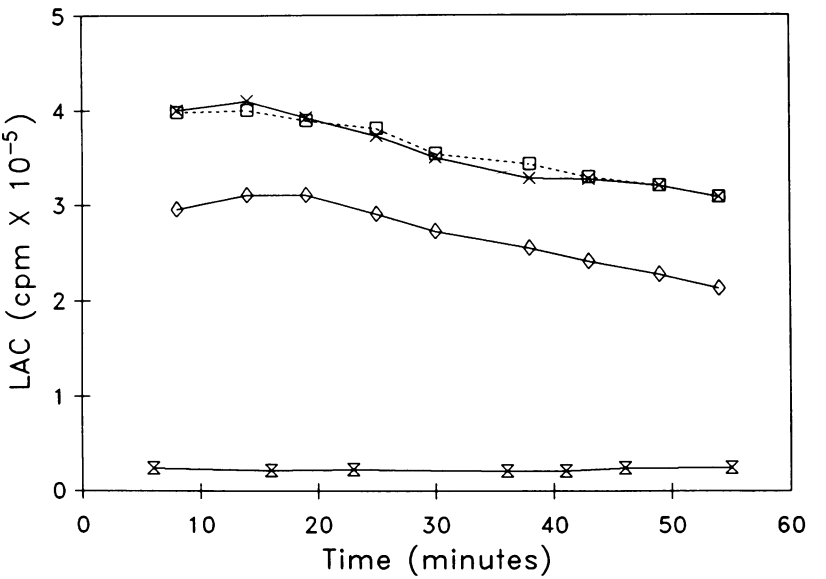

FIGURE 7

Decay of chemiluminescence counts during first 60 minutes after addition of luminol. The LAC counts were expressed as cpm/six retinas and choroids. (—×———×—, group 1), (--□-----□--, group 2), and (—◇———◇—, group 3) are decay curves from three groups of tissue samples, each containing six retinas and choroids from EAU animals collected 12 days postimmunization. The variation in LAC counts between groups was indicated by the difference between group 1 and group 3, or group 2 and group 3. The reproducibility in the kinetics of disappearance of radicals was indicated by the decay curves of group 1 and group 2. The LAC counts of the control group, also containing six retinas and choroids, during first 60 minutes is shown as group 4 (— ⧖——— ⧖—); mean ± SD (n = 3).

deferoxamine, an iron chelating agent (Fig 11). These in vitro scavenging experiments were carried out with a parallel counting procedure. Two counting vials (each containing six retinas and choroids) were first counted for a short period of time to stabilize the counts as well as to ensure that the two vials began with the same level of counts before the inhibitor was added to one vial. A brief exposure to room light during the addition procedure generally caused an immediate surge in counts, expect in the case of deferoxamine (Fig 11), where the surge was offset by a large suppressive effect. In these experiments, vials with and without the inhibitor were exposed to room light for the same period of time. The suppression of counts by the scavengers is usually immediate, and the magnitude suppression of the original counts, once stabilized, stayed the same thereafter, resulting in parallel decay curves throughout the entire

counting period (Figs 9 to 11). Without the addition of inhibitor, these two vials would follow exactly the same course of radical decay as demonstrated by the upper two curves in Fig 7.

Addition of 4500 U of SOD, a scavenger for superoxide, resulted in suppression of 120,000 to 130,000 counts, amounting to approximately 20% of the original counts before scavenger was added (Fig 9). Introduction of a second dose of 5400 U of SOD did not cause any further suppression in LAC counting. With the addition of 10 mM of D-mannitol, a hydroxyl radical scavenger, the LAC counts were decreased 150,000 counts throughout the entire counting cycles, and this magnitude amounted to 25% of the maximal counts before addition of mannitol (Fig 10). As in the case of SOD, a dose of 20 mM D-mannitol gave no further suppression. Catalase, an inhibitor for H_2O_2, did not cause a significant effect on LAC counts at doses of either 11,000 U or 20,000 U. Deferoxamine mesylate, an effective iron chelator,[28] at a concentration of 10 mM caused a decrease of 105,000 counts, 33% of the original counts prior to its

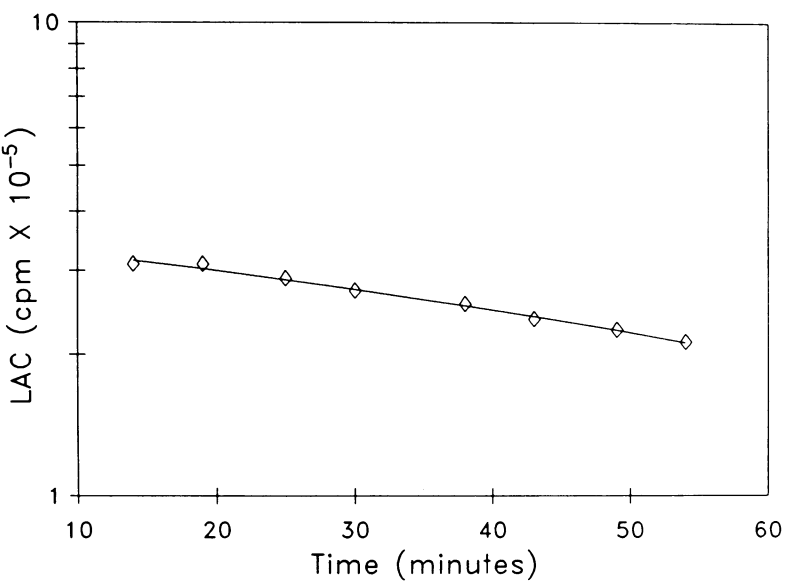

FIGURE 8
Kinetics of decay of LAC counts in first 60 minutes after addition of luminol. The logarithm of LAC counts in cpm/six retinas and choroids was plotted against time. The tissue samples were obtained from EAU animals 12 days post injection with S-antigen.

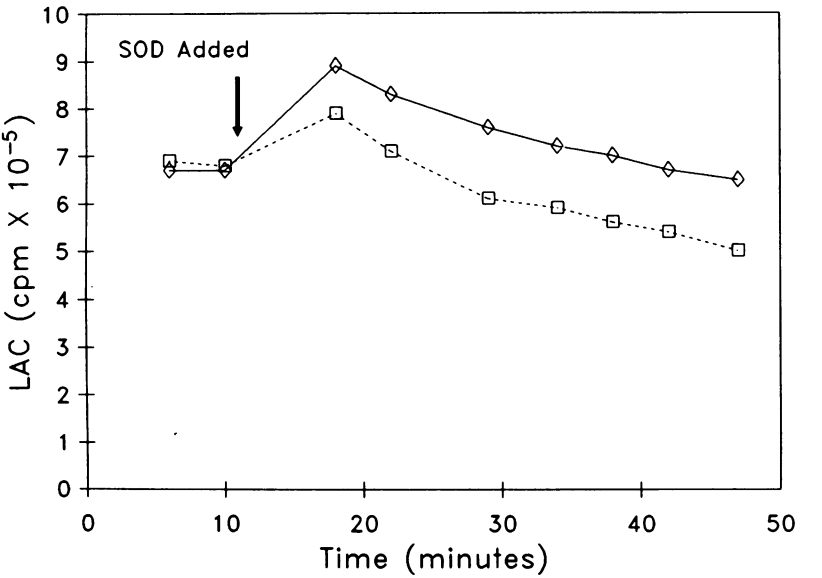

FIGURE 9
The effect of SOD on the LAC from retina and choroid of EAU animals. Chemiluminescence expressed as cpm/six retinas and choroids is shown as (—◇———◇—) from EAU animals (--□-----□--) from EAU animals, whose tissues received 5400 U of SOD. SOD was added immediately after counts were stabilized. The experiments were carried out in duplicate and a representative curve is shown here. The slight increase in counts immediately following the addition of SOD is due to a brief exposure of vials to light during the addition.

addition. This was the maximum effect obtainable for deferoxamine, as indicated by the absence of further inhibition with increased concentration (20 mM) of this agent. In nonsensitized control animals, the changes in LAC counts following addition of SOD, D-mannitol, catalase and deferoxamine mesylate were found to be insignificant.

The generation of free radicals, as measured by LAC counts, was followed during the development of uveitis, starting from the day of clinical onset of the disease. These experiments were conducted in triplicate utilizing a total of 18 globes for each time period. The time periods used were day of S-antigen injection, and days 9, 12, 15, 18, and 19 after S-antigen injection. As shown in Fig 12, on day 9 postimmunization, the LAC counts increased to only 1.5-fold that of day 0. However, the counts increased rapidly to a maximum of 18-fold on day 12 and decreased slowly thereafter. At day 19, the counts were down to about threefold that of the control level. At the point of maximal free radical activity (day 12), the

LAC counts appeared to be highly uniform between animals, demonstrated by a much smaller standard deviation; whereas on days 15 and 18, the standard deviations were larger, in the order of 100,000 counts. At day 9 and day 19, the standard deviations were invariably small, mainly because of the lower counts.

MEASUREMENT OF CONJUGATED DIENES, MALONDIALDEHYDE, AND FLUORESCENT CHROMOLIPIDS

For detecting the extent of lipid peroxidation in retinal membranes during the course of EAU development, biochemical parameters including CD, MDA, and fluorescent chromolipids were measured at time intervals similar to those used in the LAC experiments, except the initial measurements were started earlier, 7 days postsensitization. As indicated

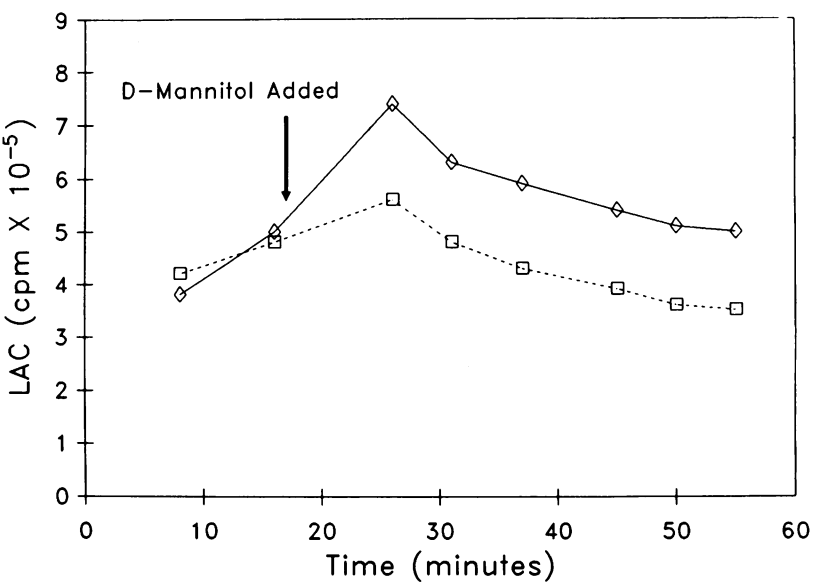

FIGURE 10

The effect of D-mannitol on the LAC from retina and choroid of EAU animals. Chemiluminescence expressed as cpm/six retinas and choroids is shown as (—◇———◇—) from EAU animals and (--□-----□--) from EAU animals plus 10 mM D-mannitol. D-mannitol was added immediately after counts were stabilized. The experiments were carried out in duplicate and a representative curve is shown here. Note the slight increase in counts immediately following the addition of D-mannitol is due to a brief exposure of vials to light during the addition.

earlier, the clinical onset of disease has been established to be at day 9 after immunization. The detection of lipid peroxidation at day 7 was attempted to determine whether lipid peroxidation is detectable before clinical signs of the disease. For each measurement in these categories, two retinas and choroids were used and the measurements were all done in triplicate. The results for CD, MDA, and fluorescent chromolipid measurements are shown in Figs 13, 14, and 15, respectively. In CD measurement, the lipid "end absorption" at 233 nm[113] was expressed as control level, 7.5 nmole/retina plus choroid. The amount of CD increased rapidly from day 7 to day 12, peaked on day 12 to 2.7-fold that of the control level and decreased slowly thereafter. The MDA measurements

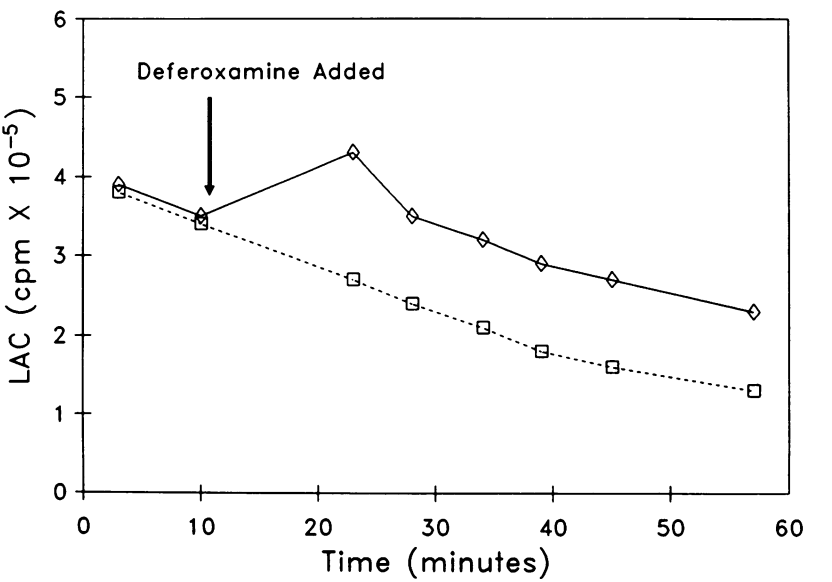

FIGURE 11

The effect of deferoxamine on the LAC from retina and choroid of EAU animals. Chemiluminescence expressed as cpm/six retinas and choroids as shown as (—◇———◇—) from EAU animals and (--□-----□--) from EAU animals plus 10 mM deferoxamine mesylate. Deferoxamine mesylate was added immediately after counts were stabilized. The experiments were carried out in duplicate and a representative curve is shown here. Immediately following the addition of scavengers, there usually is a brief surge of counts due to the exposure of counting vials to light. This is seen only in inflamed tissues without deferoxamine. With deferoxamine, this surge is offset by a large decrease in counts immediately following the addition.

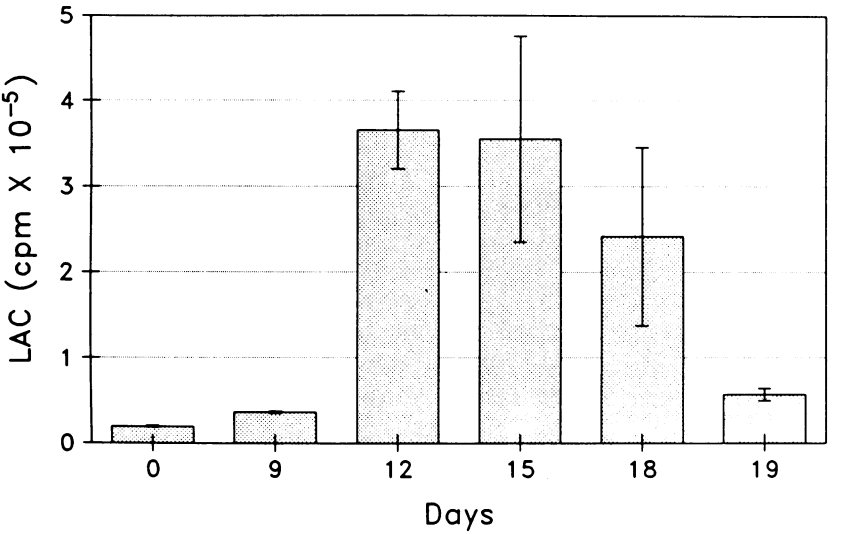

FIGURE 12
The time course of chemiluminescence as a function of EAU development. The LAC was measured at various time intervals following immunization and was expressed as cpm/six retinas and choroids. Results are shown as mean ± SD (n = 3) using zero time point as the control level.

revealed this product at low levels in uninflamed retina and choroid. The levels increased rapidly to a maximum on day 15, then fell rather rapidly to a level even lower than that of the control. The production of fluorescent Schiff base products was slightly delayed compared with the other two parameters. At day 9 the control level was still maintained. A sharp increase to a maximum was recorded on day 12, followed by a decrease in the formation of these products (Fig 15). At the maximum, on day 12, the increase in CD production above the control level (13 nmoles/eye) was much higher than was that of MDA (1 nmole/eye).

DETECTION OF HYDROPEROXIDES

The production of hydroperoxides in inflamed retinas and choroids was detected by TLC, and a final confirmation of the fatty acid hydroperoxides was carried out by GC/MS. The total crude lipids isolated from retinas and choroids without prior chemical reduction were hydrolyzed to release fatty acid moieties, after which the fatty acids were converted to methyl esters to facilitate both thin layer and gas chromatographic manipulations.

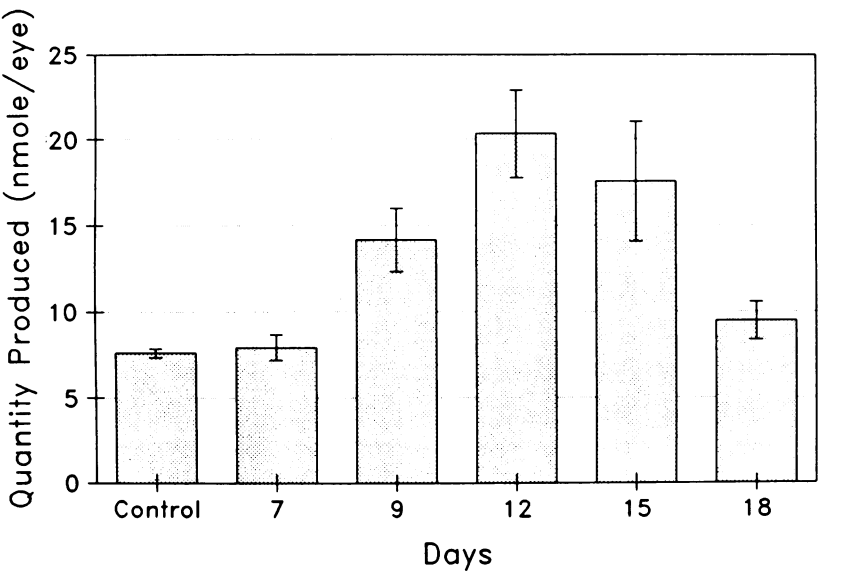

FIGURE 13
The time course of CD production during the development of EAU. The CDs were measured at various time intervals following S-antigen injection. The levels of CD are expressed as nmoles/retina and choroid. The retinas and choroids from two eyes were combined and used for one measurement. Results are shown as mean ± SD (n = 3); the control level is also included.

In Fig 16, the peroxidation products isolated from inflamed retinas and choroids (channel 3) were compared with those obtained from controls (channel 2). The identification of individual spots, in particular the hydroperoxy (region B) and hydroxy fatty acid methyl esters (region C), was carried out by comparison with the oxidation products obtained from soybean phosphatidylcholine (channel 1). Commercial soybean phosphatidylcholine was air-oxidized and transesterified by METH-PREP II as in the case of tissue samples. In all three channels without $NaBH_4$ reduction, the hydroperoxide-derived hydroxy esters (region C) are seen as more intense spots than the hydroperoxides (region B). The transesterification using a methanolic alkaline solution, as in this case, has been shown also to convert hydroperoxides to hydroxy compounds.[96] In EAU animals (channel 3), the same type of reduction is also known to be carried out endogenously by glutathione peroxidase. The hydroxy esters from soybean phosphatidylcholine, presumably mostly hydroxyoctadecadien-

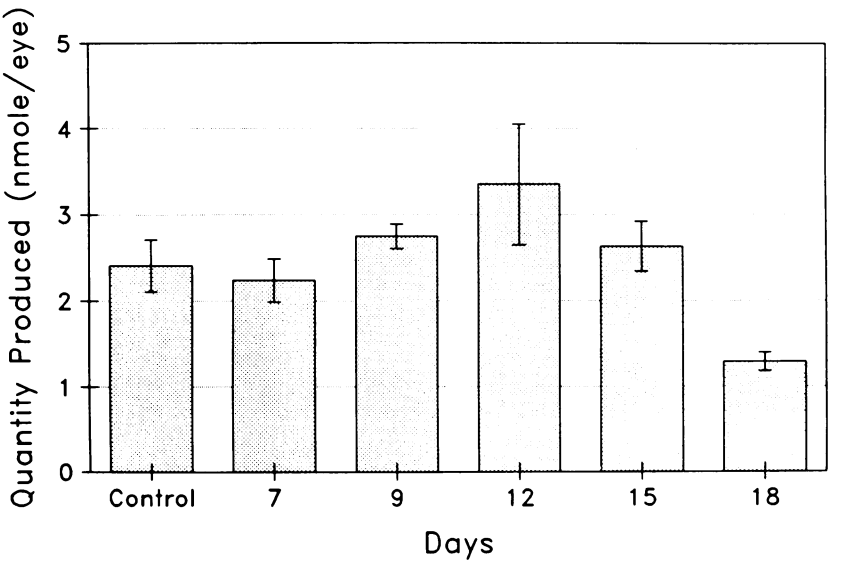

FIGURE 14
The time course of MDA production during the development of EAU. The quantities of MDA in the retinas and choroids were measured at various time intervals following S-antigen injection and MDA levels are expressed as nmoles/retina and choroid. Results are shown as mean ± SD (n = 3) and retinas and choroids from two eyes were combined for a single measurement. The control level is also included.

oic acid,[114] appear as multiple spots (region C) with R_f values between 0.23 and 0.18 (Fig 16, channel 1). The hydroxy esters from EAU animals gave similar R_f values, 0.23 to 0.17 as indicated in channel 3, region C. In the control animals without immunization (channel 2, Fig 16), no significant quantities of hydroxy fatty acids were detected in region C.

In the peroxidation of 22:6, ten possible positional isomers of hydroperoxide can be produced resulting from five skipped dienes in the molecule. Using GC/MS, with single ion monitoring, five hydroperoxide derived hydroxydocosahexaenoic acids (HDHE) from EAU retinas and choroids collected 14 days after S-antigen immunization are characterized. These are 10-, 11-, 13-, 14-, and 17-HDHEs. The mass spectrometry of trimethylsilyl ether, methyl ester derivative of isometric HDHE has been well documented recently by two studies.[115,116] On the high mass side, the molecular ions m/z 430, m/z 415 ($M\text{-}CH_3$), and m/z 399 ($M\text{-}OCH_3$) appear as low intensity peaks, but are often discernible upon

computer-assisted amplification to increase intensities.[117] The intense peaks in mass spectra of HDHE result from cleavage of alpha to the trimethylsilyl group, thus confirming the presence as well as the position of the hydroxyl group in these compounds. Among the two possible modes of alpha cleavages, it appears that for all the HDHEs only one intense cleavage peak alpha to trimethylsilyl group was observed, from either the methyl or carboxyl side.[115]

In Fig 17, selected ion chromatographs of the trimethylsilyl ether, methylester derivatives of 10-, 11-, 13-, 14-, and 17-HDHEs obtained from EAU retinas and choroids are presented. For 10-HDHE, m/z 263 is the fragment resulting from alpha cleavage of trimethylsilyl group on the carboxyl side; for 11-HDHE, m/z 281 from the methyl side; for 13-HDHE, m/z 223 from the carboxyl side; for 14-HDHE, m/z 321 from the methyl side; and for 17-HDHE, m/z 361 from the methyl side. For all

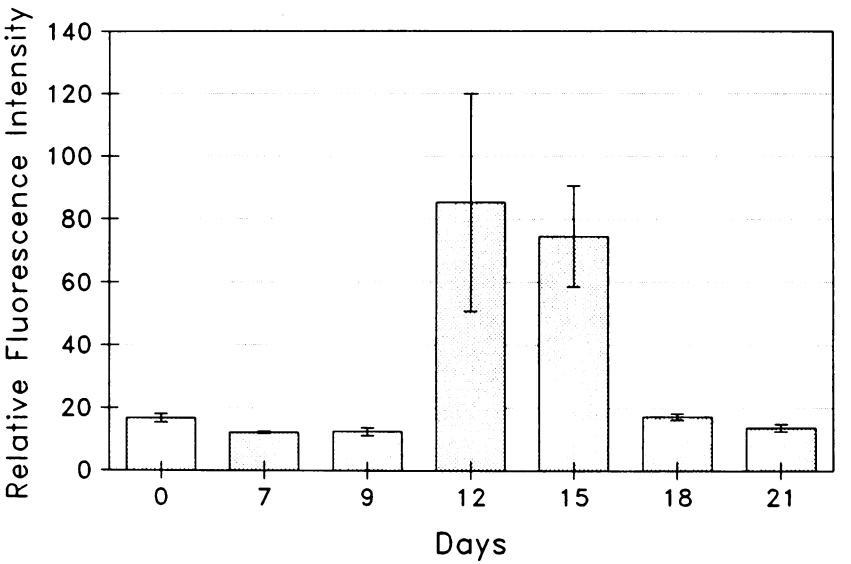

FIGURE 15

The time course of production of fluorescent Schiff base compounds during the development of EAU. The fluorescent chromolipids in the retinas and choroids were measured at various time intervals following injection of S-antigen and are expressed as relative fluorescence intensity/two retinas and choroids. Results are shown as mean ± SD (n = 3); retinas and choroids from two eyes were combined as one measurement. The control level is indicated by the value at time zero. A quinine sulfate standard (1 μg/ml of 0.1 N H_2SO_4) measured 8650 relative fluorescence units.

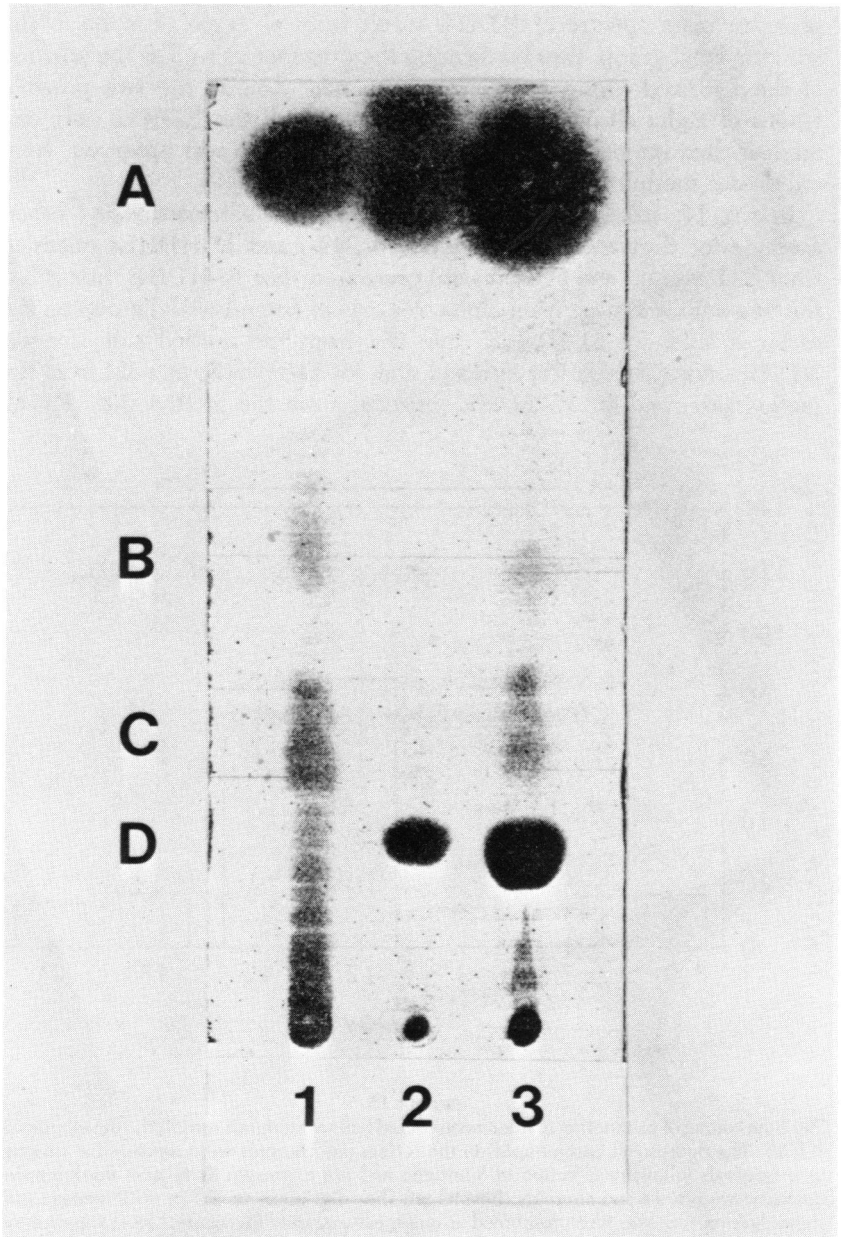
A
B
C
D
1
2
3

HDHEs identified, the m/z 430 and m/z 415 are also recognizable upon amplification in the high mass region of the total ion chromatogram.

Mass spectra were also obtained from an authentic mixture of HDHEs produced by the autoxidation of pure 22:6. Representative mass spectra from authentic HDHEs, including single ion profiles of ions 241 and 183, are shown in Fig 18. Ion 241 is the fragment ion cleaved alpha to trimethylsilyl group on methyl side for 8-HDHE, and ion 183 is the same cleavage ion on carboxyl side for 16-HDHE. The GC retention times for the authentic HDHEs were in good agreement with those from the tissue samples.

For establishing the presence of fatty acid hydroperoxide in EAU animals, five of ten possible isomers of hydroperoxide derived HDHEs were discerned by GC/MS. The other HDHEs, including 4-, 7-, 8-, 16-, and 12-HDHEs, the alpha cleavage ions, were detected only in low intensities and confirmation of these HDHEs could not be established. The possible reasons could be that: (1) these compounds are present in the tissues in smaller quantities; (2) both alpha cleavage ions are low intensity ions, as is the case of 7-HDHE[115]; or (3) the alpha cleavage ions are too small to be easily distinguishable from other ions in this region, as m/z 189 for 4-HDHE and m/z 131 for 20-HDHE.

DISAPPEARANCE OF DOCOSAHEXAENOIC ACID

In establishing the occurrence of lipid peroxidation in retinal membranes in EAU, the changes in fatty acid composition as well as the peroxidative loss of substrate, in particular 22:6, were also examined. In Fig 19A, the total fatty acid isolated from the retina and choroid of EAU animals is shown; that isolated from the control animals is shown in Fig 19B. The relative quantities of methyl palmitate (16:0) have been previously shown by other investigators to remain unchanged in retinas following light and other peroxidative damages.[39-41,44] Therefore, in Fig 19A and B, the peak

FIGURE 16

Thin layer chromatogram of total fatty acid methyl esters isolated from the retina and choroid of the control and EAU animals. Fatty acid methyl esters isolated from oxidized soybean phosphatidylcholine was used as the standard. Channel 1, oxidized methyl esters from soybean phosphatidylcholine; channel 2, from the control animals; channel 3, from the EAU animals 18 days postinjection with S-antigen. A, unchanged fatty acid methyl esters; B, hydroperoxy fatty acid methyl esters; C, hydroxy fatty acid methyl esters; D, cholesterol. Note the presence of both hydroperoxides and hydroxy fatty acids in channel 1 and 3. Hydroperoxides are known to be reduced by glutathione peroxidase in the tissue or by transesterification with METH-PREP II (see Materials and Methods).

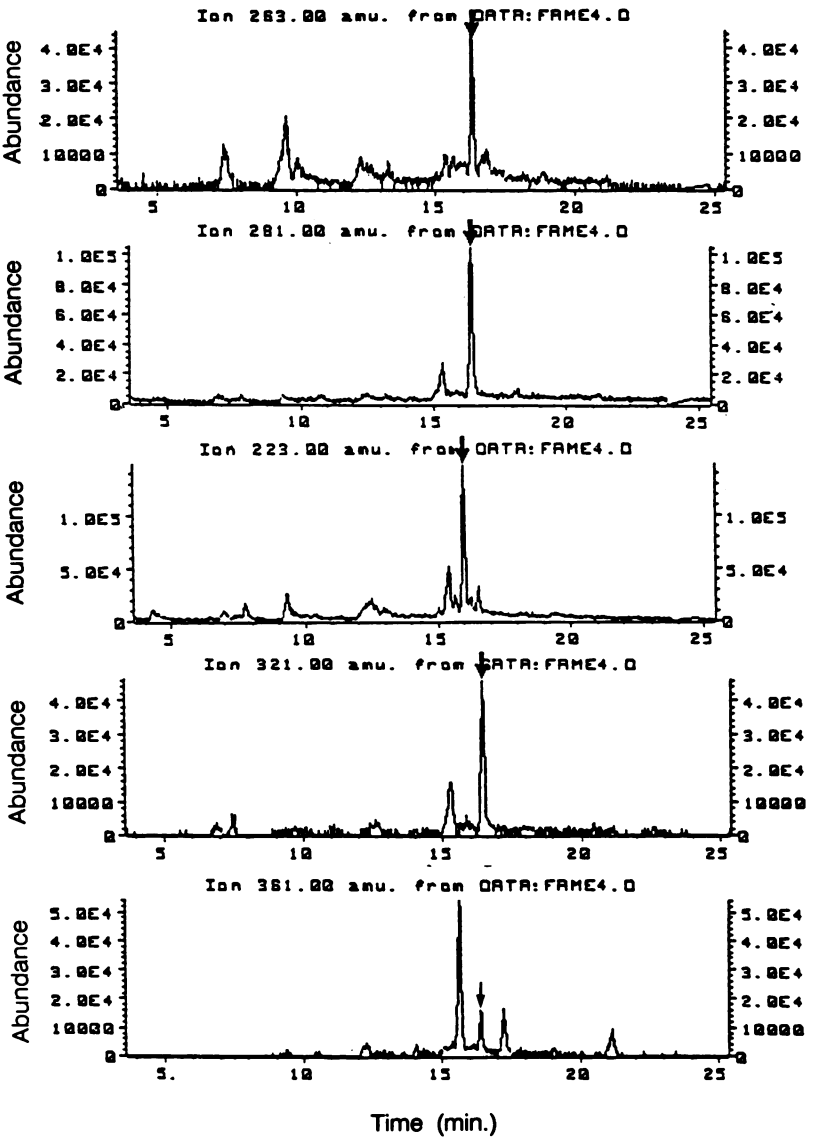

FIGURE 17
Selected ion chromatographs of the trimethylsilyl ether, methyl ester derivatives of 10-, 11-, 13-, 14-, and 17-HDHEs (m/z 263, 281, 223, 321, and 361, respectively) isolated from the retinas and choroids of EAU animals. Ion profiles of HDHEs are presented as relative peak areas.

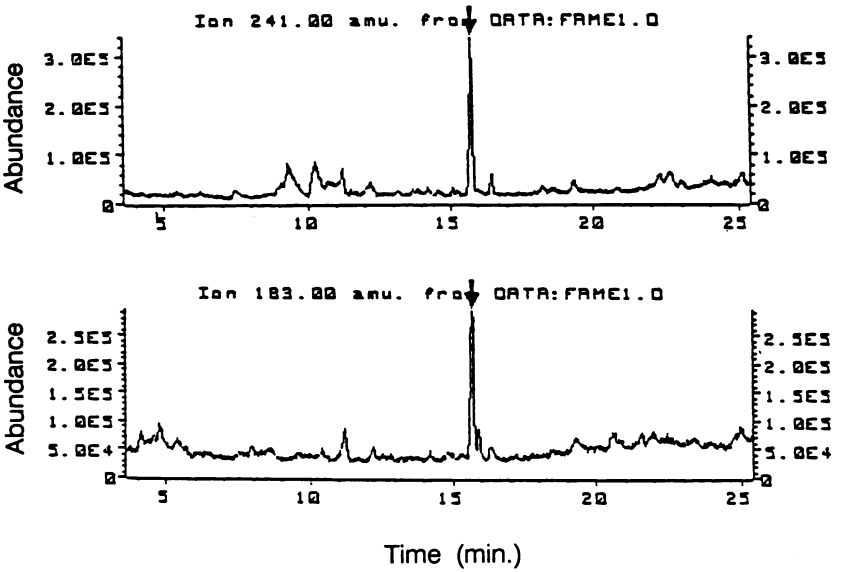

FIGURE 18
Selected ion chromatographs of the trimethylsilyl ether, methyl ester derivatives of 8- and 16-HDHEs (m/z 241 and 183, respectively) isolated from autoxidized authentic 22:6. Ion profiles of HDHEs are presented as relative peak areas.

heights of 16:0 were adjusted to the same level. A significant decrease of 22:6 in EAU animals (Fig 19A) was noted as compared with that in controls (Fig 19B). Some increases in other unsaturated fatty acids, especially 20:4, are also apparent.

SUPPRESSION OF UVEITIS IN ANIMALS TREATED WITH HYDROXY RADICAL SCAVENGER (DEFEROXAMINME MESYLATE)

Clinically, all animals injected with S-antigen developed signs of intraocular inflammation on day 12 or 13. Histopathologically all animals treated with normal saline and all animals treated with ion-saturated deferoxamine showed marked inflammatory cell infiltration in the retina and choroid (Fig 20A). There was perivasculitis as well as fibrinoid necrosis of retinal vessels. The photoreceptor cells were destroyed. In contrast to these animals, rats treated with deferoxamine mesylate showed mild mononuclear cell infiltration in the retina and choroid (Fig 20B). The retinal necrosis and photoreceptor cell damage was minimal. The mor-

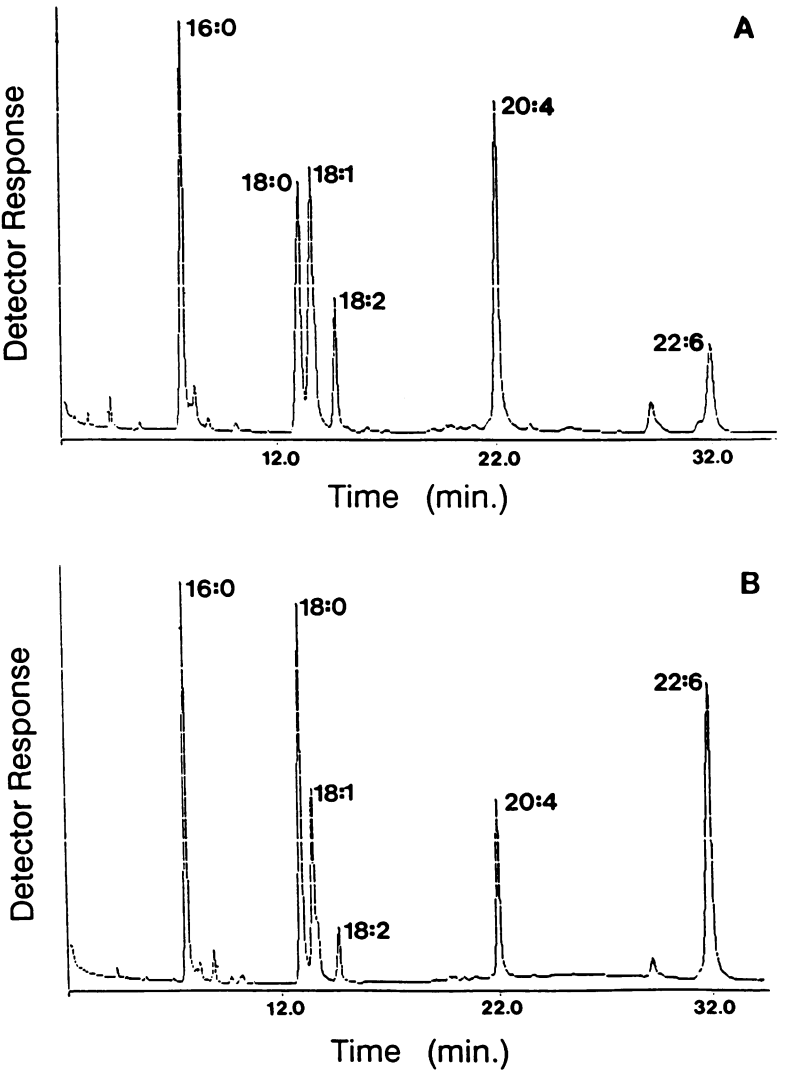

FIGURE 19
Gas chromatogram of total unchanged fatty acid methyl esters obtained from retinas and choroids of control and EAU animals. Fatty acid pattern from EAU animals is shown in A, and controls in B. Fatty acid methyl esters were identified according to the gas liquid chromatography reference standard obtained from Nu Chek Prep, Inc, Elysian, MN.

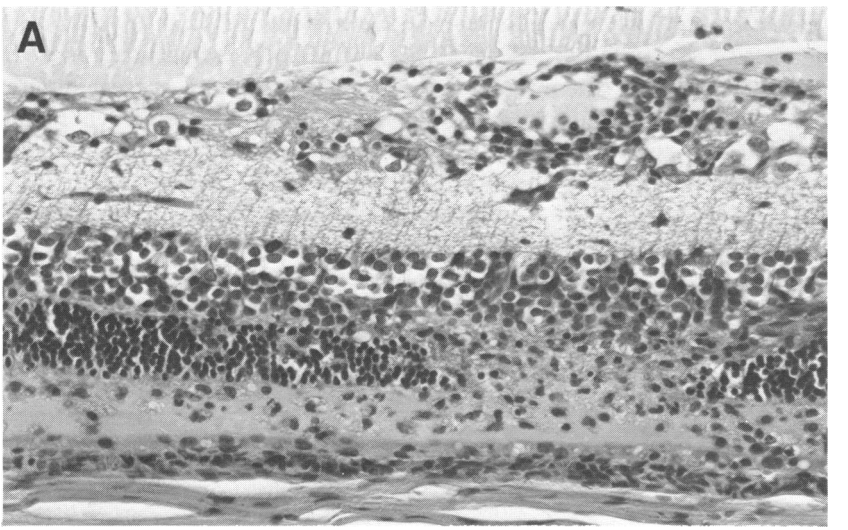

FIGURE 20
EAU animal treated with normal saline shows retinal vasculitis and retinitis with destruction of photoreceptors (A). Note presence of inflammatory cells in the retina and choroid (H&E, ×500). EAU animal treated with deferoxamine mesylate exhibits mild retinitis with infiltration of occasional inflammatory cells in the outer retina (B). Note relatively well preserved photoreceptors (H&E, ×500).

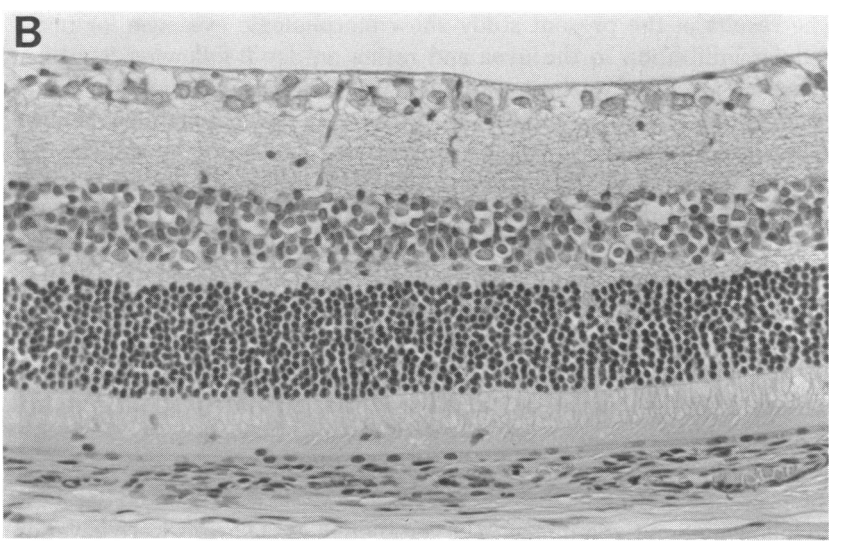

phometric analysis revealed choroidal thickness of 62.0 ± 5.1 μ in animals treated with normal saline, 58.5 ± 8.7 μ in animals treated with iron-saturated deferoxamine, and 28.7 ± 4.2 μ in animals treated with deferoxamine. Student's *t*-test revealed significant reduction of choroidal thickness in animals treated with deferoxamine compared to animals treated with normal saline or with iron-saturated deferoxamine ($P < 0.01$). There was no significant difference between the groups tested with normal saline or iron-saturated deferoxamine (Table II). The thickness of choroid in animals without uveitis was 12.3 ± 0.5 μ (Table I). The reduction in uveal inflammation in deferoxamine treated animals (based on choroidal thickness measurement) was about 68%.

TABLE II: ANIMALS TREATED WITH HYDROXYL RADICAL SCAVENGER, DEFEROXAMINE MESYLATE SHOWED MARKED REDUCTION IN UVEITIS

EXPERIMENTAL GROUPS	NO. OF ANIMALS	CHOROIDAL THICKNESS (μ)	*P* VALUE*
Treated with normal saline	6	62.0 ± 5.1	
Treated with iron-saturated deferoxamine mesylate	6	58.5 ± 8.7	
Treated with deferoxamine mesylate	6	28.7 ± 4.2	< 0.01

*Student's *t*-test comparing deferoxamine mesylate group with other two groups.

DISCUSSION

The results of the present study show morphologic evidence for initial cellular infiltration in the uvea and retina on day 9 following S-antigen injection. On this day, there was damage to the retinal cell membranes as demonstrated by ultrastructural studies (Fig 3). Even though biochemical evidence for a sparse leukocytic infiltration, evidenced by slightly elevated levels of MPO, was noted on day 7, significantly higher levels of infiltration became apparent on day 9. On this day there was considerable evidence for generation of free radicals, as measured by LAC, and presence of lipid peroxidation products in the inflamed tissue, consisting of elevated levels of CD, MDA, and fluorochrome lipids. At the same time there was retinal tissue damage noted by light and electron microscopic studies. This concurrent generation of free radicals at the site of uveoretinitis, formation of lipid peroxidation products, and development of retinal damage indicate a direct relationship between these events.

Variations in choroidal thickness reflect the severity of the uveitis.[20] In the present experiment the choriod was markedly thickened on day 12 to 15 following S-antigen injection. Even though MPO levels were lower on

day 15 than on day 12, morphologic studies showed the choroid to be thickened from inflammatory cells. The increased thickness of the choroid on day 15 appears to be from infiltration of mononuclear cells rather than PMNs (Fig 2). From this morphologic data, it appears that macrophages may play an important role in generation of free radicals during this period, whereas PMNs release these metabolites during the early phase of uveitis.

Electron microscopic studies conducted on the enucleated eyes at various time periods showed initial damage from infiltrating cells to be mostly around the retinal vessels and photoreceptors. This damage of retinal cells was prominent adjacent to the infiltrating inflammatory cells (Fig 3). These findings suggest that free radical mediated damage is limited to the immediate vicinity of their generation. Such in vivo findings from electron microscopy confirm in vitro studies demonstrating the limited capacity of free radical migration due to their high reactivity with various tissue elements at the site of their generation.

In the present study, the oxygen metabolite and hydroxyl radical generation in uveitis was supported by the histochemical methods used to detect superoxide and hydrogen peroxide production at the site of uveoretinitis. The NBT method showed the presence of superoxide in choroidal inflammation when blue formazan reaction product was evident at this site (Fig 5). The specificity of superoxide detection by this method was demonstrated when the reaction was prevented by a complex of deferoxamine mesylate and MnO_2. This complex was reported to exhibit SOD-like activity and was shown to scavenge intracellular and extracellular superoxide.[91] Lack of inhibition of superoxide by SOD was not surprising, as this large molecule cannot enter into the cells and thus is incapable of scavenging intracellular superoxide.

Ultrastructural histochemical studies utilizing cerium ion for detection of hydrogen peroxide in the tissue provided evidence for the presence of this oxygen metabolite at the site of intraocular inflammation. Ultrastructural studies showed electron dense granular material (indicative of H_2O_2) mainly around the phagocytic cells and at the site of retinal damage (Fig 6). This implicates oxygen metabolites as a cause of retinal damage and suggests an in vivo role of these oxidants in intraocular inflammation.

During the course of oxidative chain reaction, low levels of light are emitted by excited oxygen species. Such luminol amplified emission of light is referred to as chemiluminescence. The addition of luminol to chemiluminescence measurement is known to amplify detection of light. Such luminol amplified emission is found to be a sensitive assay for the production of free radicals.[118,119] Chemiluminescence in biological mate-

rial can also arise from reactions associated with peroxidation of lipid membranes and the resulting radicals.[120] However, Dowling et al[94] successfully utilized LAC for characterization of the nature of the reactive oxygen species generated in inflamed dermal tissue by using scavengers for oxygen metabolites. Utilizing this method, with minor modifications, it was possible to demonstrate generation of oxygen metabolites at the site of uveoretinitis. The identified metabolic products consisted mostly of superoxide anion and hydroxyl radicals. These results provide additional evidence for a role of these metabolites in initiating the tissue damage seen in uveitis. Such findings also substantiate the mechanism for the beneficial findings noted in in vivo treatment experiments.[20,24-27] In these treatment studies, animals with S-antigen induced uveitis or animals with phacoantigenic uveitis were intraperitoneally injected with various antioxidant enzymes, such as SOD, catalase, glutathione peroxidase, or hydroxyl radical scavengers. Such treatment resulted in significant reduction in the severity of uveitis and in the extent of retinal damage.[20] The protective effect offered by these scavengers was assumed to be from scavenging oxygen metabolites at the site of their generation in the uvea.[20,24-27] Thus, these previous treatment experiments and the present LAC method demonstrating the presence of free radicals (Figs 9 to 11) at the site of uveitis provide clear support for the generation of these cytotoxic products in the inflamed tissue and the damage they incite in the retina.

The histochemical investigations revealed the presence of H_2O_2 in the inflamed uvea and retina, but the LAC method failed to detect significant quantities of this oxidant when catalase was used as an H_2O_2 scavenger. Even though there is no clear explanation as to why the LAC method failed to detect H_2O_2, such experimental results indicate the importance of utilizing multiple methods for detection of these oxidants.

Oxygen free radicals of biologic interest are extremely reactive and unstable. As a result of the high reactivity, they have a very short half-life. Hydroxyl radicals derived from superoxide and hydrogen peroxide are known to react with a variety of biological molecules, including lipids of cell membranes and cellular DNA. Peroxidation of the PUFAs of membrane lipids can lead to breakdown of the membrane secretory functions and transmembrane ionic gradients.[121-123] Such alterations can result in cellular edema, degeneration, and necrosis. In experimental uveitis, there is ample evidence for formation of lipid peroxidation products. These products include CD, MDA products, fluorochrome Schiff base compounds, hydroperoxides, and others (Figs 13 to 17).

The initial step in free radical medicated lipid peroxidation has been

reported to be removal of a hydrogen atom from one of the methylene groups of the carbon chain, a process that leaves behind an unpaired electron on this carbon atom and creates a lipid carbon radical.[122] The lipid carbon radicals are known to rapidly undergo molecular rearrangement to produce CD. The CD rapidly react with molecular oxygen and yield hydroperoxyl radicals, which in turn abstract the hydrogen atom from a methylene carbon of an adjacent PUFA to form another lipid radical and lipid hydroperoxide. The lipid radical then reacts with another molecular oxygen and continues the chain reaction.[122] The hydroperoxyl radicals have also been demonstrated to form malonaldehyde or MDA. Malonaldehyde is known to be highly reactive with amino groups of proteins, and forms conjugated Schiff bases with characteristic fluorochromes. Based on such available information, determination of CD, MDA products, hydroperoxides, and fluorochrome products was conducted in the present study. In experimental uveitis, all of these products were detected in the inflamed retina and choroid, thus providing evidence for tissue damage from oxygen free radicals generated at the site of chorioretinal inflammation.

There are several techniques that have been employed to measure lipid peroxidation products in cell membranes. It has been mentioned that no one method by itself can be considered an accurate measure of lipid peroxidation.[123] For instance, measurement of CD is useful in early stages of the peroxidation process, but substances such as heme proteins, purines and pyrimidines are known to accelerate the decomposition of CDs and lipid hydroperoxides, and can thus create high backgrounds in spectrophotometric measurements. This can result in grossly inaccurate measurements of lipid peroxidation. Other investigators have utilized the thiobarbituric acid test to measure products arising from the decomposition of lipid hydroperoxide as a measure of lipid peroxidation. This method has also been found to be nonspecific and subject to error.[123] Because of such nonspecificity, it has been suggested that attempts should be made to measure several products of lipid peroxidation in order to establish its occurrence in a given tissue.[34,37] By utilizing several conventional methods as well as a novel GC/MS technique, the presence of various products of lipid peroxidation in the retina were demonstrated. In particular, the occurrence of fatty acid hydroperoxides in general was first detected by the TLC method, and a further structural confirmation of hydroperoxides from 22:6 was achieved by GC/MS. The approach taken in this study, and the results demonstrating various lipid peroxidation products, clearly establish oxygen free radical mediated damage in the retinal tissue. These experiments substantiate an earlier preliminary

report by Rao et al[42] on the detection of CD and MDA products in retinal tissues of animals with experimental uveitis. However, the present report also shows formation of chromolipids, hydroperoxides, and other products of lipid peroxidation in uveitis (Figs 15 to 17).

Retina, by virtue of containing abundant quantities of lipids, and in particular long chain PUFA, is especially prone to oxidative damage. The retinal photoreceptors are known to contain large amounts of 22:6. This fatty acid is markedly depleted in experimental uveitis. Similar loss of this PUFA is noted in light induced retinal degeneration, which is believed to be a free radical mediated process.[44] As the PUFA play a role in maintenance of physiologic function of photoreceptor cells, the depletion of such fatty acids could lead to loss of visual function, and to degeneration of photoreceptors and other retinal cells, similar to the changes observed in light induced retinal damage.[44] Even though the mechanisms of free radical generation are quite different in inflammation than in photic injury, the resultant tissue damage in both cases appears to involve peroxidation of retinal lipids and depletion of 22:6.

In the present experiments, both retina and choroidal tissue were used for various procedures in both experimental and control groups. Even though it was possible to separate retina from the choroid in the non-inflamed eye, this could not be achieved in animals with EAU. This was due in part to the chorioretinal adhesions and the inflammation involving both structures, including choriocapillaries and retinal pigment epithelium. The composition of the lipids isolated from the experimental animals and the controls indicated that the isolated lipids were mainly from retinal cell membranes. The general pattern of fatty acids, and the percentage of 22:6 in the isolated lipids, were similar to those reported from rod outer segment membranes.[124,125] Thus the isolated lipids and the lipid peroxidation products noted in EAU strongly indicated that these were derived from retinal tissue membranes.

Light and electron microscopic studies revealed infiltration of PMNs primarily in the initial stages of EAU. Several of these leukocytes were necrotic and were seen in the retinal layers. Such necrotic PMNs could contribute to a certain extent to the lipid peroxidation products found in the uveitis animals. However, it was less likely that cell membranes of PMNs contributed to the lipid peroxidation products noted in the EAU. Ward et al[37] and Rao et al[42] have shown absence of PMN derived lipid peroxidation products in pulmonary inflammation and in experimental uveitis. Such a lack of lipid peroxidation products from PMNs could be from abundant quantities of antioxidant enzymes and other antioxidants present in PMNs.[126,127]

Similar to the demonstration of lipid peroxidation products in experimental uveitis, other investigators have reported the occurrence of lipid peroxidation products in various systemic inflammatory diseases, including rheumatoid arthritis.[34] Ward and colleagues[37] showed the presence of CD, hydroperoxides, and fluorochrome compounds in complement mediated pneumonitis. Similar to joint or pulmonary inflammation, the inflamed retina in EAU showed presence of these peroxidation products. Moreover, the retinal tissue exhibited selective loss of 22:6. Such loss of 22:6 in uveitis provides firm evidence for the role of oxygen free radicals in retinal tissue degeneration. Even though retinal functions were not evaluated in the experimental uveitis, based on results of the light damage study it can be deduced that similar functional abnormalities should occur in experimental uveitis, as loss of 22:6 was correlated with retinal function alterations and degeneration in light-induced retinal damage.[44]

The time sequence study of retinal lipid peroxidation (Figs 13 to 15) demonstrates formation of various peroxidation products during the initial stages of uveitis. PMNs, which are an important component of the inflammatory cell infiltration in uveitis, begin to accumulate in the uvea and retina in significant numbers by day 9, as shown by the sensitive biochemical method of measuring MPO, an enzyme seen mainly in PMNs. These cells increase in number by day 12 (Fig 4). Similar to initial accumulation of PMNs, the products of lipid peroxidation are detected on day 9 and are increased markedly by day 12. Such a correlation suggests that lipid peroxidation is associated with the initial oxygen burst of PMNs. Furthermore, this time sequence also indicates that the retinal damage, in the form of peroxidation of retinal membrane lipids, occurs as an initial event in the degenerative process. This is substantiated by the finding of high levels of lipid peroxidation products seen initially on day 12, when the retina begins to show necrosis, and low levels of the peroxidation products when the retina shows marked degeneration, on day 18. This conclusion is further strengthened by the observation of loss of 22:6 in the initial phase of uveitis.

Chemiluminescence assay, which measures generation of oxygen free radicals, demonstrates the highest levels of chemiluminescence counts on day 12 following S-antigen injection. These high counts correlate well with large numbers of PMNs in the eye, as measured by MPO levels. However, when the chemiluminescence counts were compared with MPO levels at other time points, there appeared to be a lack of correlation between these two parameters (Figs 4 and 12). Such a difference may in part be due to variation in the severity of disease in various groups of animals or, more likely, could be due to antioxidant enzymes present in

the retina that may have suppressed the chemiluminescence. Several investigators have reported the presence of antioxidant enzymes such as SOD, catalase, and glutathione peroxidase in the retina.[45-48] These enzymes, along with other antioxidants present in the retina, may help in scavenging oxygen free radicals. This scavenging effect may be prominent in the initial stage of inflammation but may not be as effective in removing radicals during the later stages. It is possible that the scavenging ability of these antioxidants initially, and loss of their scavenging function later on in the inflammation, may be reflected by persistent high levels of free radical generation on day 15 and 18, despite a marked reduction in the infiltrating PMNs on these days.

The morphologic findings of minimal retinal degeneration during early phases of inflammation, when maximum quantities of free radicals are generated, suggest that the lipid peroxidation products formed from the action of free radicals on the retinal cell membranes could be the initial insult and, subsequently, lead to further damage to the retinal cells by chain reaction of lipid peroxidation and lipid radical generation (Figs 1 to 3). In addition to this mechanism, it is possible that the lipid peroxidation products could play a role in perpetuation of inflammation via their chemotactic properties. The lipid peroxidation products generated in vitro from 22:6 PUFA were found to be chemotactic for PMNs.[128] This same study shows that peroxidated lipids unrelated to prostaglandins may possess a chemotactic function.[128] In vivo it is possible that both the lipid peroxides and hydroperoxides of the retina, prostaglandins and other agents may be involved in the amplification of uveoretinitis (Fig 1). These observations explain the antiinflammatory properties of antioxidants and hydroxyl radical scavengers. The beneficial effects of antioxidant enzymes and free radical scavenger treatment could be from minimizing the generation of lipid peroxidation chemotactic factors, in addition to reducing lipid radicals.

Several investigators have suggested the following criteria for confirming a particular type of injury caused by free radicals[7,122]: (1) demonstration of abnormal production of free radicals at the site of tissue damage by electron spin resonance spectroscopy or, failing that, by chemical methods or by finding reaction products; (2) dissimilar mechanisms for producing free radicals at the sites of tissue injury should produce similar lesions; and (3) free radical scavengers should provide protection against the lesion. In the experimental S-antigen induced uveitis, all of these criteria could be met (Table III). The retinal and choroidal tissue of animals with S-antigen induced uveitis show histochemical, ultrastructural and chemical evidence of the presence of oxygen metabolites. Both superoxide and

H_2O_2 could be detected in the inflamed ocular tissue. Moreover, resultant reaction products, namely lipid peroxidation products, are noted in the inflamed tissues. Such lipid peroxidation products are generally considered as specific reaction products formed by interaction of oxygen metabolites with the lipids. These experiments, and the demonstration of protection shown by treatment experiments[20,24-27] in which antioxidant enzymes and hydroxyl radical scavengers were used in animals with S-antigen induced uveitis, clearly fulfill all three requirements needed to show that oxygen free radicals play a role in the retinal damage observed in virtually all of the animals with experimental uveitis (Table III).

TABLE III: CRITERIA FOR FREE RADICAL INDUCED TISSUE DAMAGE IN EAU

GENERAL CRITERIA OF FREE RADICAL MEDIATED DAMAGE	FINDINGS OF FREE RADICAL MEDIATED DAMAGE IN EAU
1. Abnormal production of free radicals demonstrated by:	
a. Electron spin resonance	Electron spin resonance findings in EAU are not known. Chemiluminescence in EAU shows free radical generation
b. Chemical methods	NBT and cerium histochemical methods shown superoxide and H_2O_2 generation
c. Reaction products	Lipid peroxidation products including hydroperoxides and loss of 22:6 PUFA
2. Dissimilar mechanism should produce similar lesion	Photic injury leads to similar biochemical changes of formations of lipid peroxidation products
3. Free radical scavengers should provide protection	Treatment experiments using antioxidant enzymes such as SOD, catalase, glutathione peroxidase and hydroxyl radical scavengers, including Na-benzoate, 2-3 dihydroxy benzoic acid, deferoxamine, dimethyl thiourea, and DMSO, offer protection

The treatment experiments with deferoxamine, an iron chelator known to interfere with generation of toxic hydroxyl radicals by superoxide and hydrogen peroxide, clearly showed beneficial effects of this agent in uveitis treatment (Fig 20). When administered prior to the development of uveitis, deferoxamine caused a marked reduction (68%) in the severity of intraocular inflammation (Table II). These experimental results confirm the reports on beneficial effects of deferoxamine therapy noted in animals with experimental uveitis and in other animal models of inflammation.[24,28] These protective effects of deferoxamine are not unique to this agent, as other hydroxyl radical scavengers can also reduce intraocular inflamma-

tion in S-antigen induced uveitis or in experimental phacoanaphylactic endophthalmitis. Rao and colleagues[18,24-27] and Marak et al,[19] showed that hydroxyl radical scavengers such as sodium benzoate, 2-3-dihydroxy benzoic acid and dimethyl thiourea can offer protection against oxygen free radical mediated damage to the retina. Similarly, these investigators showed significant reduction in severity of inflammation when animals with experimental uveitis were treated with SOD, catalase, and glutathione peroxidase. These previous reports and the present experiment with deferoxamine clearly establish the importance of oxygen free radical scavengers in suppressing the amplification of intraocular inflammation and, most importantly, these studies, and others conducted in preparation of this thesis, provide a foundation on which to develop a class of therapeutic agents with biological properties directed at scavenging toxic oxygen metabolites.

CONCLUSIONS

In conclusion, to my knowledge, the present experiments provide, for the first time, convincing evidence for in vivo generation of free radicals in experimental uveitis. These radicals produce retinal damage in spite of the presence of abundant quantities of antioxidants in ocular structures. One of the mechanisms for such damage appears to be from peroxidation of retinal lipids that are present abundantly in the cell membranes. These lipid peroxidation products occur early in the experimental uveitis and may play a major role in amplification and perpetuation of uveitis by initiating a chain reaction of lipid radical generation and by forming chemotactic agents (Fig 1). From these morphologic and biochemical studies, one can conclude that oxygen free radicals generated in experimental uveitis lead to retinal damage by peroxidation of retinal cell membranes. However, there are additional inflammatory mediators, such as proteases, prostaglandins, leukotrienes, complement products and cytokines of macrophages and lymphocytes, which could initiate and amplify the disease concurrent with free radicals in a complex inflammatory condition such as uveitis. However, treatement experiments with various antioxidant enzymes such as SOD, catalase, and glutathione peroxidase, or hydroxyl radical scavengers such as dimethyl thiourea and others show marked improvement in the signs of uveitis, significant reduction in the severity of intraocular inflammation, and protection to the retina from free radicals. The results reported in this thesis further suggest that the damage to the retina and to other tissues observed in uveitis can be prevented or minimized by administration of free radical scavengers.

Development of such antioxidants should be encouraged and appropriate clinical trials carried out to determine their usefulness in the treatment of human uveitis.

SUMMARY

It is known that the visual loss in severe uveitis is due primarily to retinal tissue damage. In order to test the hypothesis that this damage may result from oxygen free radical-induced peroxidation of retinal membrane lipids, the generation of oxygen metabolites at the site of intraocular inflammation was investigated in an animal model of uveitis induced by retinal S-antigen. The effect of these metabolites on the initiation of retinal damage was characterized by histochemical, biochemical, morphologic, and morphometric methods.

Light and electron microscopic studies at the early stage of the inflammation disclosed disorganization, degeneration, and necrosis of the photoreceptors and other retinal cells. Novel histochemical procedures demonstrated formation of superoxide and hydrogen peroxide at the site of uveoretinitis. Chemiluminescence measurements on uveoretinal tissue from these experimental animals revealed generation of superoxide anion and hydroxyl radicals. During the early phase of the uveoretinitis, concomitant with generation of the oxygen metabolites, there was peroxidation of retinal membrane lipids. The peroxidation products consisted of CD, MDA, hydroperoxides, and others. Associated with these changes was a selective depletion of the PUFA 22:6, decrease of which in the retinal composition has been shown to affect visual function. The morphologic and biochemical investigations clearly indicate that oxygen free radicals are generated at the site of uveoretinitis and that the retinal damage is mediated by peroxidation of lipids that are present in the retinal cell membranes. It would thus seem logical that such intraocular inflammation and the resultant retinal damage could be suppressed by antioxidant enzymes and oxygen free radical scavengers. These studies provide for the first time clear indication for developing new therapeutic agents that possess oxygen free radical scavenging properties, for treatment of human uveitis.

ACKNOWLEDGMENTS

The author gratefully acknowledges the assistance of Drs Guey-Shuang Wu, Hiroshi Goto and Geeta Pararajasegaram for their assistance with lipid peroxidation determinations, immunization of animals and for help in preparing the manuscript.

REFERENCES

1. O'Connor GR: Factors related to the initiation and recurrence of uveitis. XL Edward Jackson memorial lecture. *Am J Ophthalmol* 1983; 96:577-599.
2. Henderly DE, Genstler AJ, Smith RE, et al: Changing patterns of uveitis. *Am J Ophthalmol* 1987; 103:131-136.
3. Dinning WJ: The visual prognosis in chronic uveitis. *Ber Zusammenkunft Dtsch Ophthalmol Ges* 1981; 78:29-280.
4. Smith RE, Nozik RA: Cystoid macular edema and uveitis, in *Uveitis: A Clinical Approach to Diagnosis and Management*, 2nd ed, Baltimore, Williams & Wilkins, 1989, pp 108-1092.
5. Pinckard RN: The "new" chemical mediators of inflammation, in G Majno, RS Cotran, N Kaufman (eds): *Current Topics in Inflammation and Infection*. Baltimore, Williams & Wilkins, 1982, pp 38-53.
6. Ryan GB, Majno G: Acute inflammation: A review. *Am J Pathol* 1977; 86:183-276.
7. Southorn PA, Powis G: Free radicals in medicine: II. Involvement in human disease. *Mayo Clin Proc* 1988; 63:390-408.
8. Weiss SJ: Tissue destruction by neutrophils. *N Engl J Med* 1989; 320:365-376.
9. Hwang D: Essential fatty acids and immune response. *FASEB J* 1989; 3:2052-2061.
10. Marak GE Jr, Rao NA, Scott JM, et al: Antioxidant modulation of phacoanaphylactic endophthalmitis. *Ophthalmic Res* 1985; 17:297-301.
11. Johnson KJ, Varani J, Oliver J, et al: Immunologic vasculitis in beige mice with deficiency of leukocytic neutral protease. *J Immunol* 1979; 122:1807-1811.
12. McCord JM: Oxygen-derived radicals: A link between reperfusion injury and inflammation. *Fed Proc* 1987; 46:2402-2406.
13. Fridovich I: Oxygen radicals, hydrogen peroxide, and oxygen toxicity, in WA Pryor (ed): *Free Radicals in Biology*, vol 1. New York, Academic Press, 1976, pp 239-277.
14. Petrone WF, English DK, Wong K, et al: Free radicals and inflammation: Superoxide-dependent activation of a neutrophil chemotactic factor in plasma. *Proc Natl Acad Sci USA* 1980; 77:1159-1163.
15. Pryor WA: Free radical biology: Xenobiotics, cancer, and aging. *Ann NY Acad Sci* 1982; 393:1-22.
16. Crapo JD, Freeman BA, Barry BE, et al: Mechanisms of hyperoxic injury to the pulmonary microcirculation. *Physiologist* 1983; 26:170-176.
17. Weiss SJ, LoBuglio AF: Phagocyte-generated oxygen metabolites and cellular injury. *Lab Invest* 1982; 47:5-18.
18. Rao NA, Calandra AJ, Sevanian A, et al: Modulation of lens-induced uveitis by superoxide dismutase. *Ophthalmic Res* 1986; 18:41-46.
19. Marak GE Jr, Rao NA, Sevanian A, et al: Modulation of experimental phacoanaphylactic endophthalmitis with the antioxidants sodium benzoate, and 2,3-dihydroxybenzoic acid. *Ophthalmic Res* 1987; 19:120-128.
20. Rao NA, Sevanian A, Fernandez MAS, et al: Role of oxygen radicals in experimental allergic uveitis. *Invest Ophthalmol Vis Sci* 1987; 28:886-892.
21. Rao NA, Romero JL, Fernandez MAS, et al: Role of free radicals in uveitis. *Surv Ophthalmol* 1987; 32:209-213.
22. McCormick JR, Harkin MM, Johnson KJ, et al: Suppression by superoxide dismutase of immune-complex-induced pulmonary alveolitis and dermal inflammation. *Am J Pathol* 1981; 102:55-61.
23. Rehan A, Johnson KJ, Wiggins RC, et al: Evidence for the role of oxygen radicals in acute nephrotic nephritis. *Lab Invest* 1984; 51:396-403.
24. Rao NA, Romero JL, Fernandez MAS, et al: Effect of iron chelation on severity of ocular inflammation in an animal model. *Arch Ophthalmol* 1986; 104:1369-1371.
25. Rao NA, Romero JL, Sevanian A, et al: Anti-inflammatory effect of glutathione peroxidase on experimental lens-induced uveitis. *Ophthalmic Res* 1988; 20:213-219.
26. Rao NA, Fernandez MA, Sevanian A, et al: Treatment of experimental lens-induced uveitis by diemthyl thiourea. *Ophthalmic Res* 1988; 20:106-111.

27. ———: Antiphlogistic effect of catalase on experimental phacoanaphylactic endophthalmitis. *Ophthalmic Res* 1986; 18:185-191.
28. Bowern N, Ramshaw IA, Clark IA, et al: Inhibition of autoimmune neuropathological process by treatment with an iron-chelating agent. *J Exp Med* 1984; 160:1532-1543.
29. Sulavik MC, Johnson KJ, Ward PA: Neutrophil activation by soluble and insoluble agents. *Fed Proc* 1984; 43:389.
30. Klebanoff SJ: Oxygen metabolism and the toxic properties of phagocytes. *Ann Intern Med* 1980; 93:480-489.
31. Harrison JE, Schultz J: Studies on the chlorinating activity of myeloperoxidase. *J Biol Chem* 1976; 251:1371-1374.
32. Willson RL: Hydroxyl radicals and biological damage in vitro: What relevance in vivo? *Ciba Found Symp* 1978; 65:19-42.
33. Dizdaroglu M, Bergtold DS: Characterization of free radical-induced base damage in DNA at biologically relevant levels. *Anal Biochem* 1986; 156:182-188.
34. Halliwell B: Oxidants and human disease: Some new concepts. *FASEB J* 1987; 1:358-364.
35. Lewis JG, Hamilton T, Adams DO: The effect of macrophage development on the release of reactive oxygen intermediates and lipid oxidation products, and their ability to induce oxidative DNA damage in mammalian cells. *Carcinogenesis* 1986; 7:813-818.
36. Burton GW, Ingold KU: β-carotene: An unusual type of lipid antioxidant. *Science* 1984; 224:569-573.
37. Ward PA, Till GO, Hatherill JR, et al: Systemic complement activation, lung injury, and products of lipid peroxidation. *J Clin Invest* 1985; 76:517-527.
38. Kagan VE, Shvedova AA, Novikov KN, et al: Light-induced free radical oxidation of membrane lipids in photoreceptors of frog retina. *Biochim Biophys Acta* 1973; 330:76-79.
39. Wiegand RD, Giusto NM, Rapp LM, et al: Evidence for rod outer segment lipid peroxidation following constant illumination of the rat retina. *Invest Ophthalmol Vis Sci* 1983; 24:1433-1435.
40. Anderson RE, Rapp LM, Wiegand RD: Lipid peroxidation and retinal degeneration. *Curr Eye Res* 1984; 3:223-227.
41. Wiegand RD, Joel CD, Rapp LM, et al: Polyunsaturated fatty acids and vitamin E in rat rod outer segments during light damage. *Invest Ophthalmol Vis Sci* 1986; 27:727-733.
42. Rao NA, Fernandez MA, Cid LL, et al: Retinal lipid peroxidation in experimental uveitis. *Arch Ophthalmol* 1987; 105:1712-1716.
43. Jeffcoat R, James AT: The regulation of desaturation and elongation of fatty acids in mammals, in S Numa (ed): *Fatty Acid Metabolism and Its Regulation*. Amsterdam, Elsevier, 1984, pp 85-112.
44. Wheeler TG, Benolken RM, Anderson RE: Visual membranes: Specificity of fatty acid precursors for the electrical response to illumination. *Science* 1975; 188:1312-1314.
45. Armstrong D, Santangelo G, Connole E: The distribution of peroxide regulating enzymes in the canine eye. *Curr Eye Res* 1981; 1:225-242.
46. Rao NA, Thaete LG, Delmage JM, et al: Superoxide dismutase in ocular structures. *Invest Ophthalmol Vis Sci* 1985; 26:1778-1781.
47. Atalla L, Fernandez MA, Rao NA: Immunohistochemical localization of catalase in ocular tissue. *Curr Eye Res* 1987; 6:1181-1187.
48. Atalla LR, Sevanian A, Rao NA: Immunohistochemical localization of glutathione peroxidase in ocular tissue. *Curr Eye Res* 1988; 7:1023-1027.
49. Collins RC: Experimental studies on sympathetic ophthalmia. *Am J Ophthalmol* 1949; 32:1687-1699.
50. Silverstein AM, Zimmerman LE: Immunogenic endophthalmitis produced in the guinea pig by different pathogenetic mechanisms. *Am J Ophthalmol* 1959; 48:435-447.
51. Aronson SB, Hogan MJ, Zweigart P: Homoimmune uveitis in the guinea pig: I. General concepts of auto- and homoimmunity, methods, and manifestations. *Arch Ophthalmol* 1963; 69:105-109.

52. Wacker WB, Lipton MM: Experimental allergic uveitis: Homologous retina as uveitogenic antigen. *Nature* 1965; 206:253-254.
53. Meyers RL: Experimental allergic uveitis: Induction by retinal rod outer segments and pigment epithelium. *Mod Probl Ophthalmol* 1976; 16:41-50.
54. Wong VG, Green WR, Kuwabara T, et al: Homologous retinal outer segment immunization in primates: A clinical and histopathological study. *Arch Ophthalmol* 1975; 93:509-513.
55. Faure JP, Dorey C, Tuyen VV, et al: Experimental autoimmune uveo-retinitis and specificity of retinal antigens. *Mod Probl Ophthalmol* 1976; 16:21-29.
56. Wacker WB, Donoso LA, Kalsow CM, et al: Experimental allergic uveitis: Isolation, characterization, and localization of a soluble uveitopathogenic antigen from bovine retina. *J Immunol* 1977; 119:1949-1958.
57. Rao NA, Wacker WB, Marak GE Jr: Experimental allergic uveitis: Clinicopathologic features associated with varying doses of S antigen. *Arch Ophthalmol* 1979; 97:1954-1958.
58. de Kozak Y, Sakai J, Thillaye B, et al: S antigen-induced experimental autoimmune uveoretinitis in rats. *Curr Eye Res* 1981; 1:327-337.
59. Nussenblatt RB, Kuwabara T, de Monasterio FM, et al: S-antigen uveitis in primates: A new model for human disease. *Arch Ophthalmol* 1981; 99:1090-1092.
60. Caspi RR, Roberge FG, Chan CC, et al: A new model of autoimmune disease: Experimental autoimmune uveoretinitis induced in mice with two different retinal antigens. *J Immunol* 1988; 140:1490-1495.
61. Marak GE Jr, Shichi H, Rao NA, et al: Patterns of experimental allergic uveitis induced by rhodopsin and retinal rod outer segments. *Ophthalmic Res* 1980; 12:165-176.
62. Schalken JJ, Winkens HJ, van Vugt AHM, et al: Rhodopsin-induced experimental autoimmune uveoretinitis in monkeys. *Br J Ophthalmol* 1989; 73:168-172.
63. Broekhuyse RM, Winkens HJ, Kuhlmann ED: Induction of experimental autoimmune uveoretinitis and pinealities by IRBP: Comparison of uveoretinitis induced by S-antigen and opsin. *Curr Eye Res* 1986; 5:231-240.
64. Hirose S, Kuwabara T, Nussenblatt RB, et al: Uveitis induced in primates by interphotoreceptor retinoid-binding protein. *Arch Ophthalmol* 1986; 104:1698-1702.
65. McAllister CG, Vistica BP, Sekura R, et al: The effects of pertussis toxin on the induction and transfer of experimental autoimmune uveoretinitis. *Clin Immunol Immunopathol* 1986; 39:329-336.
66. Marak GE Jr, Font RL, Czawlytko LN, et al: Experimental lens-induced granulomatous endophthalmitis: Preliminary histopathologic observations. *Exp Eye Res* 1974; 19:311-316.
67. Meyers-Elliott RH, Gammon RA, Sumner HL, et al: Experimental retinal autoimmunity (ERA) in strain 13 guinea pigs: Induction of ERA-retinopathy with rhodopsin. *Clin Immunol Immunopathol* 1983; 27:81-95.
68. Rosenbaum JT, McDevitt HO, Guss RB, et al: Endotoxin-induced uveitis in rats as a model for human disease. *Nature* 1980; 286:611-613.
69. Broekhuyse RM, Kuhlmann ED, van Vugt AHM, et al: Immunological and immunopathological aspects of opsin-induced uveoretinitis. *Albrecht von Graefes Arch Klin Exp Ophthalmol* 1987; 225:45-49.
70. Zimmerman LE, Silverstein AM: Experimental ocular hypersensitivity: Histopathologic changes observed in rabbits receiving a single injection of antigen into the vitreous. *Am J Ophthalmol* 1959; 48:447-465.
71. Kaplan HJ, Diamond JG, Brown SA: Vitrectomy in experimental uveitis: II. Method in eyes with protein-induced uveitis. *Arch Ophthalmol* 1979; 97:336-339.
72. Howes EL Jr, Cruse VK: The structural basis of altered vascular permeability following intraocular inflammation. *Arch Ophthalmol* 1978; 96:1668-1676.
73. Bhattacherjee P, Henderson B: Inflammatory responses to intraocularly injected interleukin 1. *Curr Eye Res* 1987; 6:929-934.
74. Kulkarni PS, Srinivasan BD: Cachectin: A novel polypeptide induces uveitis in the rabbit eye. *Exp Eye Res* 1988; 46:631-633.

75. Ben-Zvi A, Rodrigues MM, Gery I, et al: Induction of ocular inflammation by synthetic mediators. *Arch Ophthalmol* 1981; 99:1436-1444.
76. Rosenbaum JT, Samples JR, Hefeneider SH, et al: Ocular inflammatory effects of intravitreal interleukin 1. *Arch Ophthalmol* 1987; 105:1117-1120.
77. Rosenbaum JT, Howes EL Jr, Rubin RM, et al: Ocular inflammatory effects of intravitreally-injected tumor necrosis factor. *Am J Pathol* 1988; 133:47-53.
78. Samples JR, Rubin RM, Wilson DJ, Rosenbaum JT: Ocular inflammatory effects of interleukin 2. *Invest Ophthalmol Vis Sci* (ARVO abstract) (Suppl) 1989; 30:441.
79. Gamble CN, Aronson SB, Brescia FB: Experimental uveitis: I. The production of recurrent immunologic (Auer) uveitis and its relationship to increased uveal vascular permeability. *Arch Ophthalmol* 1970; 84:321-330.
80. Sery TW, Petrillo R: Superoxide anion radical as an indirect mediator in ocular inflammatory disease. *Curr Eye Res* 1984; 3:243-252.
81. Mittag TW, Hammond BR, Eakins KE, et al: Ocular response to superoxide generated by intraocular injection of xanthine oxidase. *Exp Eye Res* 1985; 40:411-419.
82. Faure JP: Autoimmunity and the retina. *Curr Top Eye Res* 1980; 2:215-302.
83. Gery I, Mochizuki M, Nussenblatt RB: Retinal specific antigens and immunopathogenic processes they provoke. *Prog Ret Res* 1986; 5:75-109.
84. Nussenblatt RB, Gery I, Ballintine EJ, et al: Cellular immune responsiveness of uveitis patients to retinal S-antigen. *Am J Ophthalmol* 1980; 89:173-179.
85. Marak GE Jr, Rao NA: Retinal 's' antigen disease in rats. *Ophthalmic Res* 1982; 14:29-39.
86. Nussenblatt RB, Rodrigues MM, Wacker WB, et al: Cyclosporin A: Inhibition of experimental autoimmune uveitis in Lewis ratws. *J Clin Invest* 1981; 67:1228-1231.
87. Mochizuki M, Kuwabara T, McAllister C, et al: Adoptive transfer of experimental autoimmune uveoretinitis in rats: Immunopathogenic mechanisms and histologic features. *Invest Ophthalmol Vis Sci* 1985; 26:1-9.
88. Dorey C, Cozette J, Faure JP: A simple and rapid method for isolation of retinal S antigen. *Ophthalmic Res* 1982; 14:249-255.
89. Hirsch JG, Church AB: Studies of phagocytosis of group A streptococci by polymorphonuclear leucocytes in vitro. *J Exp Med* 1960; 111:309-322.
90. Williams RN, Paterson CA, Eakins KE, et al: Quantification of ocular inflammation: Evaluation of polymorphonuclear leukocyte infiltration by measuring myeloperoxidase activity. *Curr Eye Res* 1983; 2:465-470.
91. Ryer-Powder JE, Forman HJ: Adhering lung macrophages produce superoxide demonstrated with desferal-Mn (IV). *Free Rad Biol Med* 1989; 6:513-518.
92. Briggs RT, Drath DB, Karnovsky ML, et al: Localization of NADH oxidase on the surface of human polymorphonuclear leukocytes by a new cytochemical method. *J Cell Biol* 1975; 67:566-586.
93. Trush MA, Wison ME, Van Nyke K: The generation of chemiluminescence by phagocytic cells. *Methods Enzymol* 1978; 57:462-494.
94. Dowling EJ, Symons AM, Parke DV: Free radical production at the site of an acute inflammatory reaction as measured by chemiluminescence. *Agents Actions* 1986; 19:203-207.
95. Folch J, Lees M, Sloane-Stanley GH: A simple method for the isolation and purification of total lipides from animal tissues. *J Biol Chem* 1957; 226:497-509.
96. O'Brien PJ: Intracellular mechanisms for the decomposition of a lipid peroxide: I. Decomposition of a lipid peroxide by metal ions, heme compounds, and nucleophiles. *Can J Biochem* 1969; 47:485-492.
97. Buege JA, Aust SD: Microsomal lipid peroxidation. *Methods Enzymol* 1978; 52:302-310.
98. Ursini F, Bonaldo L, Maiorino M, et al: High-performance liquid chromatography of hydroperoxy derivatives of stearoyllinoleoylphosphatidylcholine and of their enzymatic reduction products. *J Chromatogr* 1983; 270:301-308.
99. Bergström S, Wintersteiner O: Autoxidation of sterols in colloidal aqueous solution: The nature of the products formed from cholesterol. *J Biol Chem* 1941; 141:597-610.

100. Smith LL, Kulig MJ, Teng JI: Sterol metabolism: XXVI. Pyrolysis of some sterol allylic alcohols and hydroperoxides. *Steroids* 1973; 22:627-635.
101. Uchiyama M, Mihara M: Determination of malonaldehyde precursor in tissues by thiobarbituric acid test. *Anal Biochem* 1978; 86:271-278.
102. Gutteridge JMC: The use of standards for malonyldialdehyde. *Anal Biochem* 1975; 69:518-526.
103. Sinnhuber RO, Yu TC, Yu TC: Characterization of the red pigment formed in the 2-thiobarbituric acid determination of oxidative rancidity. *Food Res* 1958; 23:626-634.
104. Jordan RA, Schenkman JB: Relationship between malondialdehyde production and arachidonate consumption during NADPH-supported microsomal lipid peroxidation. *Biochem Pharmacol* 1982; 31:1393-1400.
105. Dillard CJ, Tappel AL: Fluorescent damage products of lipid peroxidation. *Methods Enzymol* 1984; 105:337-341.
106. Shimasaki H, Ueta N, Privett OS: Isolation and analysis of age-related fluorescent substances in rat testes. *Lipids* 1980; 15:236-241.
107. Van Kuijk FJGM, Thomas DW, Stephens RJ, et al: Gas chromatography-mass spectrometry method for determination of phospholipid peroxides: Transesterification to form methyl esters. *Free Rad Biol Med* 1985; 1:215-225.
108. McCreary DK, Kossa WC, Ramachandran S, et al: A novel and rapid method for the preparation of methyl esters for gas chromatography: Application to the determination of the fatty acids of edible fats and oils. *J Chromatogr Sci* 1978; 16:329-331.
109. Bradley PP, Priebat DA, Christensen RD, et al: Measurement of cutaneous inflammation: Estimation of neutrophil content with an enzyme marker. *J Invest Dermatol* 1982; 78:206-278.
110. *Worthington Enzyme Manual*. Freehold, NJ, Worthington Biochemical Corp, 1972, pp 43-45.
111. Mullane KM, Kraemer R, Smith B: Myeloperoxidase activity as a quantitative assessment of neutrophil infiltration into ischemic myocardium. *J Pharmacol Methods* 1985; 14:157-167.
112. Ormrod DJ, Harrison GL, Miller TE: Inhibition of neutrophil myeloperoxidase activity by selected tissues. *J Pharmacol Methods* 1987; 18:137-142.
113. Recknagel RO, Glende EA Jr: Spectrophotometric detection of lipid conjugated dienes. *Methods Enzymol* 1984; 105:331-337.
114. Wu GS, Stein RA, Mead JF: Autoxidation of phosphatidylcholine liposomes. *Lipids* 1982; 17:403-413.
115. Van Rollins M, Murphy RC: Autooxidation of docosahexaenoic acid: Analysis of ten isomers of hydroxydocosahexaenoate. *J Lipid Res* 1984; 25:507-517.
116. Hughes H, Smith CV, Horning EC, et al: High-performance liquid chromatography and gas chromatography-mass spectrometry determination of specific lipid peroxidation products in vivo. *Anal Biochem* 1983; 130:431-436.
117. Van Rollins M, Baker RC, Sprecher HW, et al: Oxidation of docosahexaenoic acid by rat liver microsomes. *J Biol Chem* 1984; 259:5776-5783.
118. Pekoe G, Van Dyke K, Peden D, et al: Antioxidation theory of non-steroidal anti-inflammatory drugs based upon the inhibition of luminol-enhanced chemiluminescence from the myeloperoxidase reaction. *Agents Actions* 1982; 12:371-376.
119. Totter JR, Castro de Dugros E, Riveiro C: The use of chemiluminescent compounds as possible indicators of radical production during xanthine oxidase action. *J Biol Chem* 1960; 235:1839-1842.
120. Cadenas E, Sies H: Low-level chemiluminescence as an indicator of singlet molecular oxygen in biological systems. *Methods Enzymol* 1984; 105:221-231.
121. Barber AA, Bernheim F: Lipid peroxidation: Its measurement, occurrence, and significance in animal tissues. *Adv Gerontol Res* 1967; 2:355-403.
122. Southorn PA, Powis G: Free radicals in medicine: I. Chemical nature and biologic reactions. *Mayo Clin Proc* 1988; 63:381-389.
123. Halliwell B, Gutteridge JMC: Lipid peroxidation: A radical chain reaction, in *Free Radicals in Biology and Medicine*. Oxford, England, Clarendon Press, 1985, pp 139-189.